NATIONAL ADVISORY COMMITTEE FOR AERONAUTICS

TECHNICAL MEMORANDUM 1401

DIRECTIONAL STABILITY OF TOWED AIRPLANES

By W. Söhne

Translation of "Die Seitenstabilität eines geschleppten Flugzeuges."
Deutsches Ingenieur-Archiv, vol. 21, no. 4, 1953.

Washington
January 1956

NATIONAL ADVISORY COMMITTEE FOR AERONAUTICS

TECHNICAL MEMORANDUM 1401

DIRECTIONAL STABILITY OF TOWED AIRPLANES*[1]

By W. Söhne

1. STATEMENT OF THE PROBLEM

So far, very careful investigations have been made regarding the flight properties, in particular the static and dynamic stability, of engine-propelled aircraft and of untowed gliders. Thereby the mechanical work of airplane control was considerably facilitated for the pilot; he obtained a certain assurance in case of operating errors, and he was enabled to do blind flying. Furthermore, it became possible for the airplane designer to predetermine with certainty the stability of an airplane he was about to develop, on the basis of theory, and to influence that stability by constructive measures.

In contrast, almost no investigations exist[2] regarding the stability of airplanes towed by a towline. With the freight gliders known in Germany, a glider train is usually unstable. A towed airplane does not automatically hold to the flight path behind the towing airplane; on the contrary, its pilot must continually and carefully observe the towing airplane and balance path deviations by control deflections. Evidence for the imperfect stability of a glider train is also provided by the fact that blind towed flight of long duration is impossible. If the

---

*"Die Seitenstabilität eines geschleppten Flugzeuges." Deutsches Ingenieur-Archiv, vol. 21, no. 4, 1953, pp. 245-265. Extract from the dissertation of the author (Braunschweig 1947). Principal reviewer: Prof. Dr. H. Schlichting; coreviewer: Prof. Dr. H. Blenk.

[1]As a pilot of freight gliders in the second world war, the author was able to collect detailed flight experiences which stimulated him to undertake the theoretical investigations here described. They were performed after the end of the war, with the permission of the British Ministry of Supply, in collaboration with the Institut für Strömungsmechanik der Technischen Hochschule Braunschweig.

[2]The only report to which the author had access, by H. Solf (Die Seitenstabilität eines geschleppten Flugzeuges, FB-Bericht 1306, 1940), considered the directional stability of an airplane, the towing point of which was assumed to lie in a vertical straight line through the center of gravity, and the yawing oscillations of which were neglected. The results seem therefore not sufficiently applicable for the purposes of practice.

towing airplane is lost sight of, the pilot of the towed airplane is forced usually after a few seconds to release the towline. Even brief temporary inattentiveness may lead to badly disturbed flight positions. In flight with undisturbed view and in calm air, corrections for disturbances are performed partially intuitively and the pilot of the towed airplane becomes hardly conscious of them. In the case of squally weather, however, a high degree of attentiveness is necessary; for freight gliders, in addition, tiring manipulation of the controls is required.

The disturbed motions occur in the following two forms:

1. As a longitudinal oscillation (periodic deviations of the flight path upward and downward). It can be observed if the pilots of gliders and freight gliders are inexperienced, and is, in part, caused by too violent elevator deflections. An experienced pilot has no difficulties in eliminating these disturbed motions, except in blind flight or in low-speed flight with far-rearward position of the center of gravity.

2. As a self-excited lateral displacement oscillation which is coupled with a rolling and yawing motion. This lateral displacement oscillation appears particularly pronounced in freight gliders in the case of high wing loading. It considerably impedes the work of the pilot and may cause the towline to break, or force its release in special flight attitudes, for instance, in low-speed or in climbing flight.

Thus, the following report will aim at investigating the directional stability of the towed airplane and, particularly, at determining what parameters of the flight attitude and what configuration properties affect the stability. The most important parameters of the flight attitude are the dynamic pressure, the aerodynamic coefficients of the flight attitude, and the climbing angle. Among the configuration properties, the following exert the greatest influence on the stability: the tow-cable length, the tow-cable attachment point, the ratio of the wing loadings of the towing and the towed airplanes, the moments of inertia, and the wing dihedral of the towed airplane (which is a decisive factor in determining c_{l_β}). In addition, the size and shape of the towed airplane vertical tail, the vertical-tail length, and the fuselage configuration are decisive factors in determining c_{n_β} and c_{y_β}, the yawing moment and side force due to sideslip, respectively.

For an untowed airplane, the longitudinal and directional stability cannot be pushed so far that the airplane automatically holds to a certain flight altitude and to a certain course; likewise, a towed airplane can hardly be required to hold automatically to the flight path behind

the towing airplane, especially for the changing conditions of take-off, climbing and cruising flight. Rather, one must strive to relieve the pilot of the towed airplane as much as possible of the work of control. For blind flying, one must attempt to make orientation by the direction of the towline possible - unless an instrument can be developed which would show the position of the towed airplane with respect to the towing airplane from cable direction and cable tension.

2. INFLUENCE OF TOWED FLIGHT ON TOWING AIRPLANE AND FREIGHT GLIDER ON THE BASIS OF FLIGHT EXPERIENCES

The effect of the towing connection on the towing airplane is entirely different from the effect on the towed airplane. The towing airplane is more stable in towed than in untowed flight. It can fly more slowly, its control effectiveness is of longer duration, and disturbances are damped more rapidly. Consider, for comparison, a kite. The kite is stabilized by the drag and the mass of its long tail. The effect of a controlled towed airplane on the towing airplane is similar.

In contrast to the towing airplane, the towed airplane becomes unstable in towed flight. Calculation and flight experiences, in accordance, show that this instability increases with increasing lift coefficient, increasing wing loading, and increasing climbing angle. The ratio of the wing loadings, thus the ratio of the mutual lift coefficients, play therein an important role. For reasons of efficiency, it would be desirable that both airplanes fly at lift coefficients corresponding to their optimum glide ratios. For obtaining equal behavior in the case of squally weather[3], it would be desirable, in contrast, that the lift coefficients should be about equal. The experiences of practical flight operation, however, showed as the most favorable ratio of wing loadings of the towing airplane and of the towed airplane, with consideration of the flight properties in towed flight, approximately the value 1.6. For this ratio of wing loadings, the pilot of the towing airplane - in order to maintain soaring ability himself - must always fly so fast that the lift coefficient of the towed airplane does not exceed the value 0.8. The pilot of the towed airplane does not attain a flight attitude with higher c_a values where the control effectiveness is no longer sufficient for compensating the lateral displacement oscillation and the rolling and yawing motion connected with it. The desire for a low landing speed and

---

[3]If the wing loading of a towing airplane is three times as high as that of an empty towed airplane and the two c_a values in cruising flight are 0.75 and 0.25, a vertical gust of 6.6 m/sec at 190 km/hr causes a modification of the lift coefficient Δc_a of 0.54 or 0.6 so that there results for the towing airplane a load factor in the gust of 1.72; for the towed airplane, in contrast, one of 3.2.

for a possibility of landing outside of airfields likewise leads to a lower wing loading of the towed airplane.

The pilot of the towing airplane has only a slight influence on the flight-path correction of the towed airplane. He must only observe a few fixed rules; he must, for instance, stay above the permissible minimum speed, the permissible minimum curve radius, and the permissible gliding angle at low speed. At higher c_a values, the towed airplane has a more favorable gliding angle than the towing airplane and may in a given case, if the engines are throttled, even overtake the towing airplane.

3. SETTING UP OF THE EQUATION OF MOTION

(a) Symbols

Beside the coordinate systems defined in DIN L 100, namely, the system fixed in aircraft (x_f, y_f, z_f), the system fixed relative to the flight path (x_a, y_a, z_a) and the system fixed relative to the earth (x_g, y_g, z_g), in this report the experimental system (x, y, z) is used prominently. This system may be interpreted as a combination of the system fixed in aircraft and the system fixed relative to the flight path (fig. 1).

Furthermore, G denotes the weight of the airplane, F the wing area, $b = 2s$ the span, i_x, i_y, i_z the radii of gyration, h the vertical distance between the towing point and the center of gravity (fig. 5), a the horizontal distance between the towing point and the center of gravity, l the length of the towline, and $k_s = l/s$ the relative cable length.

As aerodynamic quantities, V signifies the undisturbed flight speed, v_y the component of the disturbed speed in y-direction, ω_x, ω_y, ω_z the angular-velocity disturbances in the experimental system, α the angle of attack, β the angle of sideslip, γ the flight-path angle ($\gamma > 0$ climbing flight).

The following is generally valid: Motions are positive with the axes. Moments and forces are positive with the axes, except for c_w and c_a. These two are positive against the axes.

In the following table, we compile the form coefficients and moment coefficients known from H. Scholz and F. Wenk.[4]

[4]H. Scholz and F. Wenk, Jahrbuch 1941 der deutschen Luftfahrtforschung, p. I 159.

	Aerodynamic form coefficients of directional stability	Moment coefficients
Lift	c_a	
Lateral force due to sideslip	$c_{q\beta} = \frac{\partial c_q}{\partial \beta}$	
Lateral force due to yawing	$c_{qz} = \frac{\partial c_q}{\partial s\omega_{za}/V}$	
Lateral force due to rolling	$c_{qx} = \frac{\partial c_q}{\partial s\omega_{xa}/V}$	
Yawing moment due to sideslip	$c_{n\beta} = -\frac{\partial c_N}{\partial \beta}$	$n_\beta = \left(\frac{s}{i_z}\right)^2 c_{n\beta}$
Lateral damping	$c_{nz} = -\frac{\partial c_N}{\partial s\omega_{za}/V}$	$n_z = \left(\frac{s}{i_z}\right)^2 c_{nz}$
Yawing moment due to rolling	$c_{nx} = -\frac{\partial c_N}{\partial s\omega_{xa}/V}$	$n_x = \left(\frac{s}{i_z}\right)^2 c_{nx}$
Rolling moment due to sideslip	$c_{l\beta} = -\frac{\partial c_L}{\partial \beta}$	$l_\beta = \left(\frac{s}{i_x}\right)^2 c_{l\beta}$
Rolling moment due to yawing	$c_{lz} = -\frac{\partial c_L}{\partial s\omega_{za}/V}$	$l_z = \left(\frac{s}{i_x}\right)^2 c_{lz}$
Damping in roll	$c_{lx} = -\frac{\partial c_L}{\partial s\omega_{xa}/V}$	$l_x = \left(\frac{s}{i_x}\right)^2 c_{lx}$
	Aerodynamic form coefficients of cable force and cable moments	Cable moment coefficients
Cable force	$c_s = c_w + c_a \tan \alpha$	
Cable rolling moment	$c_{ls} = c_s \frac{h \cos \alpha + a \sin \alpha}{s}$	$l_s = \left(\frac{s}{i_x}\right)^2 c_{ls}$
Cable yawing moment	$c_{ns} = c_s \frac{-h \sin \alpha + a \cos \alpha}{s}$	$n_s = \left(\frac{s}{i_z}\right)^2 c_{ns}$

(b) General Course of a Lateral Motion

Assume a glider train flying steadily straight ahead. Due to a disturbance, the towed airplane gets into a position with respect to the towing airplane which would be characterized by the following angles (figs. 1 and 4): σ angle between the undisturbed flight direction of the towing airplane and the towline, χ angle between the projection of the x_a-axis of the towed airplane onto the $x_g y_g$-plane against the x_g-axis, β sideslip angle of the towed airplane against its flight path, μ relative wind-bank angle. The angle between the flight direction of the towing airplane and the x-axis of the towed airplane is $\psi_e = \chi \tan \gamma + \beta$. There originates an excited lateral displacement oscillation with the following relative motions with respect to the towing airplane: lateral motion v_y of the center of gravity of the towed airplane in y direction, rolling motion ω_x about the experimental longitudinal axis, yawing motion ω_z about the experimental vertical axis. These relative motions cause the following aerodynamic forces and moments, already known from the theory of directional stability of the untowed airplane:

Lateral force due to sideslip Y_β, lateral force due to yawing $Y_{\omega z}$, lateral force due to rolling $Y_{\omega x}$

Yawing moment due to sideslip N_β, lateral damping $N_{\omega z}$, yawing moment due to rolling $N_{\omega x}$

Rolling moment due to sideslip L_β, rolling moment due to yawing $L_{\omega z}$, damping in roll $L_{\omega x}$

In addition, there are the forces and moments stemming from the cable force:

Lateral cable force Y_s, cable yawing moment N_s, cable rolling moment L_s

The lateral motion of the untowed airplane is known to be characterized by the four roots of the frequency equation, namely, by the real damping-in-roll root λ_1 which determines the quickly damped aperiodic rolling motion, a conjugate-complex pair of roots $\lambda_{23} = u_{23} \pm i w_{23}$ which determines the generally damped yawing oscillation (u_{23} damping factor, w_{23} frequency factor), and the real spiral root λ_4 which determines the generally very slow aperiodic spiral motion which may be negative, that is, stable, or positive, that is, unstable.

The lateral motion of the towed airplane, in contrast, is characterized by six roots.[5] It is characterized, as in the case of the untowed airplane, by the damping-in-roll root λ_1 and the pair of yawing-oscillation roots $\lambda_{23} = u_{23} \pm iw_{23}$. In addition, one has here a further conjugate-complex pair of roots $\lambda_{45} = u_{45} \pm iw_{45}$ which characterizes the lateral center-of-gravity displacement oscillation and is almost always strongly excited (fig. 3), and a real root λ_6 which determines the static directional stability in towed flight.

In what follows, we consider mainly the lateral displacement oscillation and the static stability in towed flight.

(c) Assumptions for Setting Up the Equations of Motion

For simplification of the calculation, the following assumptions are made:

1. Since it is only to be investigated whether the disturbed motions are stable, indifferent or unstable, it suffices to assume the disturbances to be small and thus to put $\cos \mu \approx 1$, $\sin \mu \approx \mu$, $\cos \beta \approx 1$, $\sin \beta \approx \beta$.

2. As in other stability considerations, one may investigate longitudinal and directional stability separately, on the basis of flight experiences for small disturbed motions, also in the case of the towed airplane.

3. The behavior of the airplane with fixed control surfaces is investigated.

4. It is assumed that the towing airplane holds to the flight path undisturbed by the lateral motion of the towed airplane. For the pilot of the towing plane, even slight rotations about the vertical axis caused by the cable tension are clearly noticeable; he counteracts them almost automatically by hand, or they are corrected by the automatic pilot. Since, furthermore, mass and moments of inertia of the towing airplane are considerably larger than those of the towed airplane, this assumption is realized with good approximation.

5. Finally, it is assumed that the moment coefficients increase linearily with the rotational speeds ω_x and ω_z and the lateral motion v_y; this assumption is quite customary in directional-stability theory and has proved to be permissible.

---

[5]This result of the following investigations is anticipated for the sake of better understanding.

(d) Setting Up of the Differential Equations of the Lateral Motion

The general equations of motion for the towed airplane state that the vectorial sum of aerodynamic and cable forces equals the forces of inertia and that the sum of aerodynamic and cable moments equals the angular-acceleration moments. For the investigation of the lateral motion, it suffices to consider the balances of moments about the x-axis and the z-axis, and the equilibrium of forces in the y-axis. In the following formulation of the differential equations, the acceleration terms and the terms of the aerodynamic forces and moments in the form given by H. Scholz and F. Wenk[6] are used.

1. The lateral-force equation.- The mass acceleration is $(G/g)V\dot{\chi}\cos\gamma$. The aerodynamic lateral force equals $A\mu + Y_\beta + Y_{\omega x} + Y_{\omega z}$. After introduction of the aerodynamic form coefficients this expression reads

$$R_{ya\ air} = qF\left[c_a\mu + \beta c_{q\beta} + \frac{s\omega_{xa}}{V}c_{qx} + \frac{s\omega_{za}}{V}c_{qz}\right]$$

or, because of $\omega_{za} = \omega_z$, $\omega_{xa} = \omega_x - \omega_y\beta$

$$R_{ya\ air} = qF\left[c_a\mu + \beta\left(c_{q\beta} - \frac{s\omega_y}{V}c_{qx}\right) + \frac{s\omega_x}{V}c_{qx} + \frac{s\omega_z}{V}c_{qz}\right] \qquad (1)$$

In addition, one has a cable lateral force. Due to its lateral motion, the towed airplane travels longer distances than the towing airplane which is assumed to fly steadily straight ahead. Thereby, velocity differences and mass accelerations originate which find expression in variable cable forces. In order to determine variation and order of magnitude of the velocity differences and accelerations, these quantities were investigated for an oscillation obtained by flying. The result of this investigation permits considering the speed of the towed airplane as constant. Taking a climbing or descending angle γ into consideration, one then finds the cable force to be

$$S = \frac{W + A\tan\gamma}{\cos(\sigma - \chi\cos\gamma)}\cos\mu = \frac{qF(c_w + c_a\tan\gamma)}{\cos(\sigma - \chi\cos\gamma)}\cos\mu$$

After introduction of the cable-force coefficient $c_s = c_w + c_a\tan\gamma$ and because of $\cos\mu = 1$, S is

[6]See footnote 4 on p. 4.

$$S = \frac{qFc_s}{\cos(\sigma - \chi \cos \gamma)} \tag{2}$$

and the sideward cable-force component is

$$S_{ya} = S \sin (\sigma - \chi \cos \gamma) = qFc_s \tan (\sigma - \chi \cos \gamma) \tag{3}$$

Thus the lateral-force equation reads

$$\frac{G}{g}V\dot{\chi} \cos \gamma = qF\left[c_a\mu + \beta\left(c_{q\beta} - \frac{s\omega_y}{V}c_{qx}\right) + \frac{s\omega_x}{V}c_{qx} + \frac{s\omega_z}{V}c_{qz} + c_s \tan(\sigma - \chi \cos \gamma)\right] \tag{4}$$

In this equation, the variables χ, μ, β, ω_x, ω_z, and σ occur. The influence of ω_y is very slight. The quantities ω_x, ω_z, and the velocity v_{yg} in y_g-direction are chosen as variables of the differential equation. Thus the variables χ, μ, β, and σ are to be eliminated. For this purpose, there exist the following relationships:

$$\dot{\chi} \cos \gamma = \omega_z - \dot{\beta} \qquad \ddot{y}_g = \dot{v}_{yg} = V\dot{\chi} \cos \gamma = V(\omega_z - \dot{\beta})$$

$$\dot{\chi} \cos \gamma = \frac{\dot{v}_{yg}}{V} \qquad \dot{\beta} = \omega_z - \frac{\dot{v}_{yg}}{V}$$

$$\dot{\mu} - \dot{\chi} \sin \gamma + \dot{\chi} \cos \gamma \sin \mu \sin \beta = \omega_x$$

$$\dot{\mu} = \omega_x + \dot{\chi} \cos \gamma(\tan \gamma - \sin \mu \sin \beta) \approx \omega_x + \dot{\chi} \cos \gamma \tan \gamma$$

$$\dot{\mu} = \omega_x + \frac{\dot{v}_{yg}}{V} \tan \gamma$$

Furthermore, there is (fig. 4)

$$-y_g = l \sin \sigma + a \sin (\chi \cos \gamma + \beta)$$

$$\sigma = \arcsin \left[-\frac{y_g}{l} - \frac{a}{l} \sin (\chi \cos \gamma + \beta) \right]$$

$$\tan (\sigma - \chi \cos \gamma) = \tan \left\{ \arcsin \left[-\frac{y_g}{l} - \frac{a}{l} \sin (\chi \cos \gamma + \beta) \right] - \chi \cos \gamma \right\} \tag{5}$$

For this, one may put with good approximation

$$\tan (\sigma - \chi \cos \gamma) = -\left[\frac{y_g}{l} + \chi \cos \gamma \left(1 + \frac{a}{l} \right) + \beta \frac{a}{l} \right]$$

and thus

$$\frac{d}{dt} \left[\tan (\sigma - \chi \cos \gamma) \right] = -\left(\frac{v_{yg}}{l} + \frac{\dot{v}_{yg}}{V} + \omega_z \frac{a}{l} \right) \tag{6}$$

One eliminates the quantities χ, μ, β, and σ by differentiating first the lateral-force equation (4). Thus one obtains

$$\frac{G}{gqF} \ddot{v}_{yg} = c_a \left(\omega_x + \frac{\dot{v}_{yg}}{V} \tan \gamma \right) + \left(\omega_z - \frac{\dot{v}_{yg}}{V} \right) \left(c_{q\beta} - \frac{s\omega_y}{V} c_{qx} \right) + \beta \frac{s\dot{\omega}_y}{V} c_{qx} + \frac{s\dot{\omega}_x}{V} c_{qx} + \frac{s\dot{\omega}_z}{V} c_{qz} - c_s \left(\frac{v_{yg}}{l} + \frac{\dot{v}_{yg}}{V} + \omega_z \frac{a}{l} \right) \tag{7}$$

Therein the term with $\dot{\omega}_y$ is negligible.

In equation (7), the directional-stability parameters, flight-mechanical time unit $T_F = 2G/g\rho VF$ and relative airplane mass density $\mu_s = 2G/g\rho sF$, are introduced, and s/V and l/V are eliminated by means of the following relationships:

$$\frac{s}{V} = \frac{T_F}{\mu_s} \qquad k_s = \frac{l}{s} \qquad \frac{l}{V} = \frac{T_F k_s}{\mu_s}$$

Then the equation (7) is rearranged according to the variables ω_x, ω_z, and v_{yg}, and reads finally

$$-\dot{\omega}_z c_{qz}\frac{T_F}{\mu_s} - \omega_z\left(c_{q\beta} - \omega_y c_{qx}\frac{T_F}{\mu_s} - c_s\frac{a}{l}\right) - \dot{\omega}_x c_{qx}\frac{T_F}{\mu_s} - \omega_x c_a +$$

$$\frac{\ddot{v}_{yg}}{V}T_F + \frac{\dot{v}_{yg}}{V}\left(c_{q\beta} - c_a \tan\gamma + c_s - \omega_y c_{qx}\frac{T_F}{\mu_s}\right) + \frac{v_{yg}}{V}c_s\frac{\mu_s}{T_F k_s} = 0 \qquad (8)$$

2. The moment equations.- Rotary motions about the coordinate axes are determined, for the untowed airplane, by Euler's equations for rigid bodies. For the towed airplane there occurs, in addition, a coupling of the rotary motions with the lateral motion of the airplane center of gravity due to the cable lateral force and its moments. Since Euler's equations are here referred not to the main inertia system but to the experimental system, they do not appear in the simple form known but in a general form, with the left sides[7]

$$\left.\begin{aligned} U_x &\equiv J_x\dot{\omega}_x + (J_z - J_x)\frac{\tan 2\alpha}{2}\dot{\omega}_z - \omega_y\left[-\omega_x(J_z - J_x)\frac{\tan 2\alpha}{2} + \omega_z(J_y - J_z)\right] \\ U_z &\equiv J_z\dot{\omega}_z + (J_z - J_x)\frac{\tan 2\alpha}{2}\dot{\omega}_x - \omega_y\left[+\omega_x(J_x - J_y) + \omega_z(J_z - J_x)\frac{\tan 2\alpha}{2}\right] \end{aligned}\right\} \qquad (9)$$

Therein J_x, J_y, J_z signify the moments of inertia about the experimental axes. Expressed by the main inertia moments, one obtains because of $y \equiv y_f$

$$\left.\begin{aligned} J_x &= J_{xf}\cos^2\alpha + J_{zf}\sin^2\alpha \qquad J_y \equiv J_{yf} \\ J_z &= J_{xf}\sin^2\alpha + J_{zf}\cos^2\alpha \\ (J_x - J_z)\frac{\tan 2\alpha}{2} &= J_{xz} = (J_{xf} - J_{zf})\frac{\sin 2\alpha}{2} \end{aligned}\right\} \qquad (10)$$

[7] H. Scholz, Jahrbuch 1940 der deutschen Luftfahrtforschung, p. I 433.

The aerodynamic force moments L about the x-axis and N about the z-axis are composed of contributions stemming from the motions of sideslip, rolling, and yawing. They read, with use of the aerodynamic coefficients of these motions

$$L \equiv -qFs\left[\beta c_{l\beta} + \frac{s\omega_{xa}}{V}c_{lx} + \frac{s\omega_{za}}{V}c_{lz}\right]$$

$$N \equiv -qFs\left[\beta c_{n\beta} + \frac{s\omega_{xa}}{V}c_{nx} + \frac{s\omega_{za}}{V}c_{nz}\right]$$

or, because of $\omega_{za} \equiv \omega_z$ and $\omega_{xa} = \omega_x \cos\beta - \omega_y \sin\beta \approx \omega_x - \omega_y\beta$

$$\left.\begin{aligned} L &\equiv -qFs\left[\beta\left(c_{l\beta} - c_{lx}\frac{s\omega_y}{V}\right) + \frac{s\omega_x}{V}c_{lx} + \frac{s\omega_z}{V}c_{lz}\right] \\ N &\equiv -qFs\left[\beta\left(c_{n\beta} - c_{nx}\frac{s\omega_y}{V}\right) + \frac{s\omega_x}{V}c_{nx} + \frac{s\omega_z}{V}c_{nz}\right] \end{aligned}\right\} \qquad (11)$$

With the cable force (2) the lateral component of the cable force, referred to the experimental y-axis, becomes (fig. 4)

$$S_y = S \sin(\sigma - \chi\cos\gamma - \beta) = qFc_s\frac{\sin(\sigma - \chi\cos\gamma - \beta)}{\cos(\sigma - \chi\cos\gamma)}$$

For the cable rolling moment and cable yawing moment (fig. 5), there results therefore

$$L_{cable} = +qFc_s h_e\frac{\sin(\sigma - \chi\cos\gamma - \beta)}{\cos(\sigma - \chi\cos\gamma)}$$

$$N_{cable} = +qFc_s a_e\frac{\sin(\sigma - \chi\cos\gamma - \beta)}{\cos(\sigma - \chi\cos\gamma)}$$

Instead of using the quantities h_e and a_e, referred to the experimental system, the quantities may be referred to the system fixed in aircraft h and a with the transformation

$$h_e = h \cos \alpha + a \sin \alpha \qquad a_e = - h \sin \alpha + a \cos \alpha$$

and also the aerodynamic form coefficients of the cable moments c_{ls} and c_{ns} are introduced. Then the cable-moment equations read

$$\left.\begin{aligned} L_{cable} &= +qFsc_{ls}\frac{\sin (\sigma - \chi \cos \gamma - \beta)}{\cos (\sigma - \chi \cos \gamma)} \\ N_{cable} &= +qFsc_{ns}\frac{\sin (\sigma - \chi \cos \gamma - \beta)}{\cos (\sigma - \chi \cos \gamma)} \end{aligned}\right\} \tag{12}$$

With (9), (11), and (12), Euler's equations now read

$$\left.\begin{aligned} &J_x\dot{\omega}_x + (J_z - J_x)\frac{\tan 2\alpha}{2}\dot{\omega}_z - \omega_y\left[-\omega_x(J_z - J_x)\frac{\tan 2\alpha}{2} + \omega_z(J_y - J_z)\right] = \\ &-qFs\left[\beta\left(c_{l\beta} - c_{lx}\frac{s\omega_y}{V}\right) + \frac{s\omega_x}{V}c_{lx} + \frac{s\omega_z}{V}c_{lz} - c_{ls}\frac{\sin (\sigma - \chi \cos \gamma - \beta)}{\cos (\sigma - \chi \cos \gamma)}\right] \\ &J_z\dot{\omega}_z + (J_z - J_x)\frac{\tan 2\alpha}{2}\dot{\omega}_x - \omega_y\left[\omega_x(J_x - J_y) + \omega_z(J_z - J_x)\frac{\tan 2\alpha}{2}\right] = \\ &-qFs\left[\beta\left(c_{n\beta} - c_{nx}\frac{s\omega_y}{V}\right) + \frac{s\omega_x}{V}c_{nx} + \frac{s\omega_z}{V}c_{nz} - c_{ns}\frac{\sin (\sigma - \chi \cos \gamma - \beta)}{\cos (\sigma - \chi \cos \gamma)}\right] \end{aligned}\right\} \tag{13}$$

In these equations the directional-stability parameters T_F and μ_s are introduced as follows:

$$\left.\begin{aligned} \frac{J_x}{qFs} &= \frac{2Gi_x^2}{g\rho V^2 Fs} = T_F\left(\frac{i_x}{s}\right)^2\frac{s}{V} = \frac{T_F^2}{\mu_s}\left(\frac{i_x}{s}\right)^2 \\ \frac{J_z}{qFs} &= \frac{T_F^2}{\mu_s}\left(\frac{i_z}{s}\right)^2 \end{aligned}\right\} \tag{14}$$

Furthermore, the equations (13) are multiplied by $\mu_s = T_F \frac{V}{s}$ and divided by $\left(\frac{i_x}{s}\right)^2$ and $\left(\frac{i_z}{s}\right)^2$, respectively. They then assume the form

$$\left.\begin{aligned}
&\dot{\omega}_x T_F{}^2 + \left[\left(\frac{i_z}{i_x}\right)^2 - 1\right]\frac{\tan 2\alpha}{2} T_F{}^2 \dot{\omega}_z - \omega_y \left\{ - \omega_x \left[\left(\frac{i_z}{i_x}\right)^2 - 1\right]\frac{\tan 2\alpha}{2} T_F{}^2 + \right. \\
&\left. \omega_z \frac{J_y - J_z}{J_x} T_F{}^2 \right\} = - \left\{ \beta \left[c_{l\beta} \left(\frac{s}{i_x}\right)^2 \mu_s - c_{lx} \left(\frac{s}{i_x}\right)^2 T_F \omega_y \right] + \omega_x T_F c_{lx} \left(\frac{s}{i_x}\right)^2 + \right. \\
&\left. \omega_z T_F c_{lz} \left(\frac{s}{i_x}\right)^2 - \mu_s c_{ls} \left(\frac{s}{i_x}\right)^2 \frac{\sin (\sigma - \chi \cos \gamma - \beta)}{\cos (\sigma - \chi \cos \gamma)} \right\} \\
&\dot{\omega}_z T_F{}^2 + \left[1 - \left(\frac{i_x}{i_z}\right)^2\right]\frac{\tan 2\alpha}{2} T_F{}^2 \dot{\omega}_x - \omega_y \left\{ \omega_x \frac{J_x - J_y}{J_z} T_F{}^2 + \right. \\
&\left. \omega_z \left[1 - \left(\frac{i_x}{i_z}\right)^2\right] T_F{}^2 \frac{\tan 2\alpha}{2} \right\} = - \left\{ \beta \left[c_{n\beta} \left(\frac{s}{i_z}\right)^2 \mu_s - c_{nx} \left(\frac{s}{i_z}\right)^2 T_F \omega_y \right] + \right. \\
&\left. \omega_x T_F c_{nx} \left(\frac{s}{i_z}\right)^2 + \omega_z T_F c_{nz} \left(\frac{s}{i_z}\right)^2 - \mu_s c_{ns} \left(\frac{s}{i_z}\right)^2 \frac{\sin (\sigma - \chi \cos \gamma - \beta)}{\cos (\sigma - \chi \cos \gamma)} \right\}
\end{aligned}\right\} \qquad (15)$$

One simplifies these equations by introducing the moment coefficients and the influence factors of form and position of the ellipse of inertia

$$\kappa_l = \left[\left(\frac{i_z}{i_x}\right)^2 - 1\right]\frac{\tan 2\alpha}{2} \qquad \kappa_n = \left[1 - \left(\frac{i_x}{i_z}\right)^2\right]\frac{\tan 2\alpha}{2} \qquad \kappa_\alpha = \frac{1}{1 - \kappa_l \kappa_n} \qquad (16)$$

then one differentiates them in order to be able to eliminate the expressions β, χ, and σ. Because of the value σ (5) the expression at the right in (15) becomes

$$\frac{\sin\ (\sigma - \chi \cos\ \gamma - \beta)}{\cos\ (\sigma - \chi \cos\ \gamma)} =$$

$$\frac{\sin\left\{\arcsin\left[-\frac{y_g}{l} - \sin\ (\chi \cos\ \gamma + \beta)\frac{a}{l}\right] - \chi \cos\ \gamma - \beta\right\}}{\cos\left\{\arcsin\left[-\frac{y_g}{l} - \sin\ (\chi \cos\ \gamma + \beta)\frac{a}{l}\right] - \chi \cos\ \gamma\right\}}$$

For this equation one may write with close approximation

$$\frac{\sin\ (\sigma - \chi \cos\ \gamma - \beta)}{\cos\ (\sigma - \chi \cos\ \gamma)} = -\left[\frac{y_g}{l} + (\chi \cos\ \gamma + \beta)\left(1 + \frac{a}{l}\right)\right]$$

With $\omega_z = \dot{\chi} \cos\ \gamma + \dot{\beta}$ there results finally for the differentiated quotient

$$\frac{d}{dt}\left\{\frac{\sin\ (\sigma - \chi \cos\ \gamma - \beta)}{\cos\ (\sigma - \chi \cos\ \gamma)}\right\} = -\frac{v_{yg}}{l} - \omega_z\left(1 + \frac{a}{l}\right)$$

After elimination of the quantities $\dot{\beta}$, χ, and σ and introduction of the expression $V/l = \mu_s T_F k_s$, the differentiated equations (15) are rearranged and read finally

$$\left.\begin{aligned}
&\ddot{\omega}_x T_F^2 + \dot{\omega}_x T_F\left(l_x + \omega_y \kappa_l T_F\right) + \ddot{\omega}_z \kappa_l T_F^2 + \dot{\omega}_z T_F\left(l_z - \frac{J_y - J_z}{J_x}\omega_y T_F\right) + \omega_z\left[l_\beta \mu_s - l_x \omega_y T_F + l_s \mu_s\left(1 + \frac{a}{l}\right)\right] - \\
&\frac{\dot{v}_{yg}}{V}\left[l_\beta \mu_s - l_x \omega_y T_F\right] + \frac{v_{yg} l_s \mu_s^2}{V T_F k_s} + \left\{\dot{\omega}_y T_F\left[\omega_x \kappa_l T_F - \omega_z \frac{J_y - J_z}{J_x} T_F - \beta l_x\right]\right\} = 0 \\
&\ddot{\omega}_z T_F^2 + \dot{\omega}_z T_F\left(n_z - \omega_y \kappa_n T_F\right) + \omega_z\left[n_\beta \mu_s + n_x \omega_y T_F + n_s \mu_s\left(1 + \frac{a}{l}\right)\right] + \ddot{\omega}_x \kappa_n T_F^2 + \dot{\omega}_x T_F\left(n_x - \frac{J_x - J_y}{J_z}\omega_y T_F\right) - \\
&\frac{\dot{v}_{yg}}{V}\left[\mu_s n_\beta - n_x \omega_y T_F\right] + \frac{v_{yg} n_s \mu_s^2}{V T_F k_s} + \left\{\dot{\omega}_y T_F\left[\omega_z \kappa_n T_F - \omega_x \frac{J_x - J_y}{J_z} T_F - \beta n_x\right]\right\} = 0
\end{aligned}\right\} \quad (17)$$

The braces in (17) are, because of the factor $\dot{\omega}_y$, almost equal zero and are neglected later on.

In addition to the mass and angular acceleration terms $\left(\sim\dot{v}_{yg},\ \dot{\omega}_x,\ \dot{\omega}_z\right)$ and the aerodynamic forces and moments $\left(\sim v_{yg},\ \omega_x,\ \omega_z\right)$ of the differential equations of the untowed airplane, one has for the towed airplane the cable forces and moments $\left(\sim y_g\right)$.

3. Simplification of the differential equations and dimensionless representation of their variables.- The differential equations of the lateral motion contain a number of smaller quantities with ω_y and $\dot{\omega}_y$ which, generally, may be neglected. Furthermore it is useful to represent the variables ω_x, ω_z, and v_{yg} in the following - dimensionless - manner

$$\omega_x T_F = p \qquad \omega_z T_F = r \qquad \left(v_{yg}/V\right)\mu_s = v$$

$$\dot{\omega}_x T_F^2 = \dot{p} \qquad \dot{\omega}_z T_F^2 = \dot{r} \qquad \left(\dot{v}_{yg}/V\right)\mu_s T_F = \dot{v}$$

$$\ddot{\omega}_x T_F^3 = \ddot{p} \qquad \ddot{\omega}_z T_F^3 = \ddot{r} \qquad \left(\ddot{v}_{yg}/V\right)\mu_s T_F^2 = \ddot{v}$$

Neglecting the correction factors and using a dimensionless representation of the variables, one expands the three differential equations (8), (17), and the lateral-force equation, by T_F, and the last one, moreover, by μ_s; they then read

$$\left.\begin{aligned}
&\ddot{p} + \dot{p}l_x + \kappa_l\ddot{r} + \dot{r}l_z + r\mu_s\left[l_\beta + l_s\left(1 + \frac{a}{l}\right)\right] - \dot{v}l_\beta + vl_s\frac{\mu_s}{k_s} = 0\\
&k\ddot{p} + \dot{p}n_x + \ddot{r} + \dot{r}n_z + r\mu_s\left[n_\beta + n_s\left(1 + \frac{a}{l}\right)\right] - \dot{v}n_\beta + vn_s\frac{\mu_s}{k_s} = 0\\
&-\dot{p}c_{qx} - pc_a\mu_s - \dot{r}c_{qz} - r\mu_s\left(c_{q\beta} - c_s\frac{a}{l}\right) + \ddot{v} +\\
&\dot{v}\left(c_{q\beta} - c_a\tan\gamma + c_s\right) + vc_s\frac{\mu_s}{k_s} = 0
\end{aligned}\right\} \qquad (18)$$

(e) The Frequency Equation

With the statement

$$p = C_p e^{\lambda t/T_F} \qquad r = C_r e^{\lambda t/T_F} \qquad v = C_v e^{\lambda t/T_F}$$

one obtains from (18) the following characteristic equation in the form of a determinant:

$$\begin{vmatrix} \lambda^2 + \lambda l_x & \lambda^2\kappa_l + \lambda l_z + \mu_s\left[l_\beta + l_s\left(1 + \frac{a}{l}\right)\right] & -\lambda l_\beta + l_s\frac{\mu_s}{k_s} \\ \lambda^2\kappa_n + \lambda n_x & \lambda^2 + \lambda n_z + \mu_s\left[n_\beta + n_s\left(1 + \frac{a}{l}\right)\right] & -\lambda n_\beta + n_s\frac{\mu_s}{k_s} \\ -\lambda c_{qx} - c_s\mu_s & -\lambda c_{qz} - \mu_s\left(c_{q\beta} - c_s\frac{a}{l}\right) & \lambda^2 + \lambda\left(c_{q\beta} - c_a \tan\gamma + c_s\right) + c_s\frac{\mu_s}{k_s} \end{vmatrix} = 0 \qquad (19)$$

Computation of the determinant yields the following frequency equation of the sixth degree:

$$A_0\lambda^6 + A_1\lambda^5 + A_2\lambda^4 + A_3\lambda^3 + A_4\lambda^2 + A_5\lambda + A_6 = 0 \qquad (20)$$

This frequency equation is two degrees higher than that of the untowed airplane. The coefficients read, after one has multiplied them by $\kappa_\alpha = 1/(1 - \kappa_l\kappa_n)$, in order to be able to put

$$
\begin{aligned}
A_0 &= 1: \\
A_1 &= \kappa_\alpha\left[l_x + \kappa_l n_x + n_z + \kappa_n l_z\right] + c_{q\beta} - c_a \tan\gamma + \underline{c_s} \\
A_2 &= \kappa_\alpha\Big\{l_x n_z - n_x l_z + \left(c_{q\beta} - c_a \tan\gamma + \underline{c_s}\right)\left(l_x - \kappa_l n_x + n_z - \kappa_n l_z\right) - c_{qz}\left(n_\beta - \kappa_n l_\beta\right) - \\
&\quad c_{qx}\left(l_\beta - \kappa_l n_\beta\right) + \mu_s\left(n_\beta - \kappa_n l_\beta\right) + \underline{\mu_s\left(1 + \frac{a}{l}\right)\left(n_s - \kappa_n l_s\right)}\Big\} + \underline{c_s\frac{\mu_s}{k_s}} \\
A_3 &= \kappa_\alpha\Big\{\left(c_{q\beta} - c_a \tan\gamma + \underline{c_s}\right)\left(l_x n_z - n_x l_z\right) + \mu_s\left(l_x n_\beta - n_x l_\beta\right) - c_{qz}\left(l_x n_\beta - n_x l_\beta\right) - c_{qx}\left(l_\beta n_z - n_\beta l_z\right) - \\
&\quad c_a\mu_s\left(l_\beta - \kappa_l n_\beta\right) - c_a \tan\gamma\,\mu_s\left(n_\beta - \kappa_n l_\beta\right) + \underline{\mu_s\left(1 + \frac{a}{l}\right)\Big[\left(c_{q\beta} - c_a \tan\gamma + c_s\right)\left(n_s - \kappa_n l_s\right) + l_x n_s - n_x l_s + c_s\left(n_\beta - \kappa_n l_\beta\right)\Big]} + \underline{\frac{\mu_s}{k_s}\Big[\left(n_s - \kappa_n l_s\right)c_{qz} + \left(l_s - \kappa_l n_s\right)c_{qx}\Big] + \frac{c_s\mu_s}{k_s}\left(l_x - \kappa_l n_x + n_z - \kappa_n l_z\right)\Big\}} \\
A_4 &= \kappa_\alpha\mu_s\Big\{c_a\left(n_\beta l_z - l_\beta n_z\right) + \underline{\Big[c_s\left(1 + \frac{a}{l}\right) - c_a \tan\gamma\Big]\left(n_\beta l_x - l_\beta n_x\right) + \left(c_{q\beta} - c_a \tan\gamma + c_s\right)\left(1 + \frac{a}{l}\right)\left(l_x n_s - n_x l_s\right) - c_{qx}\left(1 + \frac{a}{l}\right)\left(l_\beta n_s - n_\beta l_s\right) + \frac{c_s}{k_s}\left(l_x n_z - n_x l_z\right) + \frac{c_{qx}}{k_s}\left(l_s n_z - n_s l_z\right) + \frac{c_{qz}}{k_s}\left(l_x n_s - n_x l_s\right) + \frac{\mu_s}{k_s}\Big[c_s\left(n_\beta - \kappa_n l_\beta\right) + \left(c_{q\beta} + c_s\right)\left(n_s - \kappa_n l_s\right) + c_a\left(l_s - \kappa_l n_s\right)\Big]}\Big\} \\
A_5 &= \kappa_\alpha\mu_s^2\Big\{\underline{\frac{1}{k_s}\Big[\left(c_{q\beta} + c_s\right)\left(l_x n_s - n_x l_s\right) + c_s\left(l_x n_\beta - n_x l_\beta\right) + c_{qx}\left(l_s n_\beta - n_s l_\beta\right) - c_a\left(l_z n_s - n_z l_s\right)\Big] + c_a\left(l_s n_\beta - n_s l_\beta\right)\left(1 + \frac{a}{l}\right)}\Big\} \\
A_6 &= \underline{\kappa_\alpha\mu_s^3\frac{c_a}{k_s}\left(1 + \frac{a}{l}\right)\left(l_s n_\beta - n_s l_\beta\right)}
\end{aligned}
\qquad (21)
$$

The terms not underlined yield the coefficients of the frequency equation of the untowed airplane. In addition, one has for the frequency equations of the towed airplane the underlined terms which stem from the cable forces and moments. The influence factors of the ellipse of inertia κ_l, κ_n are generally so small that they may be neglected. (See table I.)

(f) Stability Conditions of the Frequency Equation

For stability considerations, a numerical calculation of the individual roots is frequently not necessary; it suffices to determine the limits within which stability exists. The directional stability of a towed airplane is given, if all roots of the frequency equation have a

negative real part. For this, the condition[8] is valid that all coefficients and the following determinants (for the equation of the sixth degree) must be positive:

$$D_1 = A_1 \qquad D_2 = \begin{vmatrix} A_1 & A_0 \\ A_3 & A_2 \end{vmatrix} \qquad D_3 = \begin{vmatrix} A_1 & A_0 & 0 \\ A_3 & A_2 & A_1 \\ A_5 & A_4 & A_3 \end{vmatrix}$$

$$D_4 = \begin{vmatrix} A_1 & A_0 & 0 & 0 \\ A_3 & A_2 & A_1 & A_0 \\ A_5 & A_4 & A_3 & A_2 \\ 0 & A_6 & A_5 & A_4 \end{vmatrix} \qquad D_5 = \begin{vmatrix} A_1 & A_0 & 0 & 0 & 0 \\ A_3 & A_2 & A_1 & A_0 & 0 \\ A_5 & A_4 & A_3 & A_2 & A_1 \\ 0 & A_6 & A_5 & A_4 & A_3 \\ 0 & 0 & 0 & A_6 & A_5 \end{vmatrix} \qquad (22)$$

In the case of instability of the lateral displacement oscillation, only the determinant D_5 is negative. It must therefore become positive so that stability may be attained. If the determinant D_5 is computed, there results

$$A_3A_6 - A_5A_4 + \frac{A_5^2}{A_1} - \frac{\left[A_5\left(A_2 - A_3/A_1\right) - A_1A_6\right]^2}{A_1A_4 - A_5 - A_3A_2 + A_3^2/A_1} \geqq 0$$

Therein $A_1A_4 - A_5$ is small (about 1.5 percent) compared to $-A_3A_2 + A_3^2/A_1$. If the second-degree term in the numerator of this expression is expanded, the term $A_1^2A_6^2$ is likewise small compared to the preceding terms (1.5 percent). If the small terms are neglected after expansion, there results as the condition for stability of the lateral displacement oscillation

$$A_3^2A_6 - A_3A_4A_5 + A_2A_5^2 - 2A_1A_5A_6 \geqq 0 \qquad (23)$$

---

[8] H. Bilharz, Zeitschrift für angewandte Mathematik und Mechanik 21, 1941, p. 96.

An explicit representation and general discussion of this equation with use of the expressions for the individual coefficients is not possible. However, if one wants to determine the stability limits for two variables, for instance, k_s or c_a against l_β, one obtains - since the individual coefficients contain linear terms with l_β - a cubic equation from which one can calculate for every c_a and k_s the pertaining l_β.

The stability condition for static stability reads

$$A_6 = \kappa_\alpha\left(\mu_s^3/k_s\right)c_a\left(l_s n_\beta - n_s l_\beta\right) \gtrless 0$$

Consequently,

$$l_s n_\beta - n_s l_\beta \gtrless 0$$

If one replaces the moment coefficients by the aerodynamic form coefficients and factors out various constant terms, this equation reads

$$c_{n\beta}\left(\frac{h}{a} + \tan\alpha\right) - c_{l\beta}\left(-\frac{h}{a}\tan\alpha + 1\right) \gtrless 0 \qquad (24)$$

If the towing point is located in the nose on a horizontal in front of the center of gravity $\left(h_e = 0, \quad a_e > 0\right)$, there must be

$$-c_{l\beta} = +\delta c_L/\delta\beta \gtrless 0$$

This condition is to be fulfilled by a suitable dihedral. If the towing point is located above the center of gravity $\left(a_e = 0, \quad h_e > 0\right)$, there must be

$$c_{n\beta} = -\delta c_N/\delta\beta \gtrless 0$$

This condition is satisfied in the case of directional stability of the airplane. If the towing point lies at the center of gravity, static indifference results.

(g) Special Cases

Since the work involved for the determination of the coefficients and for solution of the frequency equation of the sixth degree is very high, we investigated to see whether a few special cases with a lower number of degrees of freedom could not serve as approximate solutions.

In the calculation of the motion of the center of gravity of a towed airplane without consideration of the rolling and yawing motion (one degree of freedom), thus for $\omega_x = \omega_z = 0$, there results a quadratic frequency equation, the conjugate-complex pair of roots of which characterizes the lateral displacement oscillation.

In the calculation of the center of gravity and rolling motion of a towed airplane without consideration of the yawing motion (two degrees of freedom), thus for $\omega_z = 0$, there results a frequency equation of the fourth degree, the real roots of which characterize the damping in roll and static stability in towed flight, and the conjugate-complex pair of roots of which characterizes the lateral displacement oscillation[9].

In the calculation of the center of gravity and yawing motion of a towed airplane without consideration of the rolling motion (two degrees of freedom), thus for $\omega_x = 0$, there results a frequency equation of the fourth degree, the conjugate-complex pairs of roots of which characterize the yawing oscillation and the lateral displacement oscillation.

In the calculation of the rolling and center-of-gravity motion of a towed airplane where the yawing motion is rigidly coupled with the center-of-gravity motion (two degrees of freedom), there results a frequency equation of the fourth degree, the real roots of which characterize the damping in roll and static stability and the conjugate-complex pair of roots of which characterizes the lateral displacement oscillation.

A numerical comparison of the roots of the special cases with those of the general frequency equation showed that the lateral displacement oscillation and the static stability were not reproduced even approximately correctly in a single case. The influence of the yawing motion as well as of the rolling motion on the entire directional stability is so great that none of those two may be neglected, without completely falsifying the results. Thus no approximate solutions may be found in this manner, and it remains necessary to seek the solution of the complete frequency equation of the sixth degree with all stated degrees of freedom.

---

[9]This case is identical with the calculation performed by Solf (see footnote 2, p. 1) where coupling in a vertical straight line through the center of gravity was assumed and the yawing oscillation had been neglected.

4. DETERMINATION OF THE AERODYNAMIC AND CABLE FORCES AND MOMENTS

The determination of the coefficients of the individual aerodynamic forces and moments is an important and difficult part of the calculation of directional stability. The coefficients dependent on the angle of sideslip, lateral force due to sideslip $c_{q\beta}$, rolling moment due to sideslip $c_{l\beta}$, and the directional stability $c_{n\beta}$, are obtained by six-component measurements in the wind tunnel. The influence of modifications of the wing shape and of the dihedral, of shape and length of the fuselage and of the vertical-tail surfaces area, however, can be expressed numerically in a simple form.[10] The coefficients dependent on the rolling and yawing angular velocity, yawing moment due to rolling c_{nx}, damping in roll c_{lx}, lateral damping c_{nz}, and rolling moment due to yawing c_{lz} have, so far, been obtained almost exclusively by calculation.[11] The coefficients of the lateral force due to rolling c_{qx} and of the lateral force due to yawing c_{qz} are very small and are neglected below, as having insignificant effect on the results of the calculations. The cable-force and cable-moment coefficients may be obtained numerically in a simple form. The cable lateral force c_s is a function of the aerodynamic efficiency and of the angle of climb of the towed airplane. The cable yawing moment c_{ns} and the cable rolling moment c_{ls} are, moreover, dependent on the geometrical position of the towing point with respect to the center of gravity (fig. 5). In the case of the towing point lying in the nose the cable yawing moment is the decisive factor.

---

[10] H. Scharn, Systematisch-kritische Beispielrechnungen zur Seitenstabilität des Flugzeuges, Zentrale für wissenschaftliches Berichtswesen, UM-Bericht No. 2032, 1943; H. Schlichting, Aerodynamik der gegenseitigen Beeinflussung der Flugzeugteile, Monographie des M. O. S. (A), Völkenrode, Reports and Translation No. 171 (176). Bericht 46/5 des Instituts für Strömungsmechanik der Technischen Hoschschule Braunschweig.

[11] G. Mathias, Z. Flugt. Motorluftsch., 23, (1932), p. 224; H. Henn and H. Weiler, Untersuchung über die Seitenbewegung von Flugzeugen, Vorabdruck zum Jahrbuch 1943 der deutschen Luftfahrtforschung, Technische Berichte 11 (1944), No. 3.

5. SOLUTION OF THE FREQUENCY EQUATION

In view of the complicated structure of the general frequency equation it is difficult to make statements regarding the roots of the frequency equation, and thus on the lateral motion of the towed airplane, from the coefficients or from the aerodynamic and cable force parameters. One must therefore completely calculate numerous systematic examples in order to recognize the influence of a few variables of the flight attitude and of configuration parameters on the directional stability. First Gräffe's method[12] was used for the numerical solution of the frequency equation. This method permits calculation of the roots with arbitrary accuracy. However, it is laborious and does not offer a possibility of error control in the course of the calculation. For this reason approximate solutions for determination of individual roots were looked for.

(a) Approximate Solutions for the Roots of the Frequency Equation

The numerical calculations were based on the aerodynamic and configuration data of the freight glider Go 242 (fig. 6). The coefficients and roots of the frequency equation are, for this airplane, for a flying weight of 5,500 kg, a lift coefficient $c_a = 0.436$, and a relative cable length $k_s = 6$, of the following magnitudes: $A_1 = 18.7$, $A_2 = 52.4$, $A_3 = 316.1$, $A_4 = 24.8$, $A_5 = 74.7$, $A_6 = 40.0$, damping-in-roll root $\lambda_1 = -16.7$, yawing oscillation $\lambda_{23} = -1.0 \pm 4.2i$, lateral displacement oscillation $\lambda_{45} = +0.17 \pm 0.56i$, static stability $\lambda_6 = -0.37$. For other flying weights, lift coefficients, and cable lengths, too, as also for other model types, the orders of magnitude of the individual roots show proportions similar to those of the example mentioned. Thus they are, except for the small difference between λ_{45} and λ_6, numerically very different. Hence it follows that the large roots λ_1 and λ_{23} are determined mainly by the coefficients A_1 to A_3 whereas the small roots λ_{45} and λ_6, in contrast, are determined by the coefficients A_3 to A_6 of the frequency equation. For the approximate solutions one makes use of this fact by breaking the frequency equation of the sixth degree (20) down into two cubic equations:

---

[12]F. A. Willers, Methoden der praktischen Analysis.

$$\lambda^3 + A_1\lambda^2 + A_2\lambda + A_3 = 0 \tag{25}$$

$$\lambda^3 + \frac{A_4}{A_3}\lambda^2 + \frac{A_5}{A_3}\lambda + \frac{A_6}{A_3} = 0 \tag{26}$$

From the first cubic equation (25) one calculates the large damping-in-roll root λ_1 and the pair of roots of the yawing oscillation λ_{23}, from the second cubic equation (26) the pair of roots of the lateral displacement oscillation λ_{45} and the small static-stability root λ_6.

A first approximate solution for λ_6 is obtained from (26) with the aid of a monogram; it is improved according to Horner's scheme. (Since the roots λ_{45} and λ_6 are of the same order of magnitude, the expression $\lambda_6 = -A_6/A_5$ is too inaccurate as a first approximation.)

One can then calculate $\lambda_{45} = u_{45} \pm iw_{45}$ with the aid of the Vieta relations, applied for (26). One has

$$2u_{45} + \lambda_6 = -\frac{A_4}{A_3} \qquad r_{45}^2\lambda_6 = -\frac{A_6}{A_3} \qquad w_{45} = \sqrt{r_{45}^2 - u_{45}^2} \tag{27}$$

For λ_1, Scharn[13] indicated the approximate solution

$$\lambda_1 = A_1 + \frac{A_2}{A_1} - \frac{A_3}{A_1} \tag{28}$$

This approximation is perfectly sufficient if λ_1 is considered by itself. However, since λ_1 will be required again for calculation of the other roots, it is advisable to correct λ_1 by means of the Horner scheme referred to (25).

Since all roots, except $\lambda_{23} = u_{23} \pm iw_{23}$, are known, one may employ, for determination of u_{23}, the Vieta relation for the entire frequency equation (20)

$$\lambda_1 + 2u_{23} + 2u_{45} + \lambda_6 = -A_1 \qquad u_{23} = \frac{-A_1 - \lambda_1 - \lambda_6}{2} - u_{45} \tag{29}$$

---

[13]See footnote 10 on p. 22.

Furthermore, one has approximated according to the Vieta relations for equation (25)

$$r_{23}^2\lambda_1 = -A_3 \qquad w_{23} = \sqrt{r_{23}^2 - u_{23}^2}$$

A comparison of the solutions calculated according to these approximate formulas and according to Gräffe's method showed, for a number of examples for which the lift coefficient and the dihedral were varied, the following errors of the approximate solution:

	λ_1	u_{23}	w_{23}	u_{45}	w_{45}	λ_6
Maximum error, percent	0.04	-3.7	1.2	-19.2	2.9	-4.2
Mean error, percent	.02	-2.9	1.1	-16.6	1.7	-1.4

The agreement is satisfactorily exact except for the error in the excitation of the lateral displacement oscillation u_{45}. For some investigations these approximate solutions are, therefore, not sufficient. One can considerably improve them by expanding for λ_6 Horner's scheme by two stages of (20), and for λ_1 by three stages (to include the entire equation (20)). One may improve the values of the conjugate-complex pairs of roots $r_{45}^2 = -A_6/A_3\lambda_6$ and $r_{23}^2 = -A_3/\lambda_1$ by replacing A_3 by a corrected $\overline{A_3}$ for which the following relation is valid:

$$\overline{A_3} = A_3 - \frac{1}{A_3}\left(A_2A_4 - 0.97A_1A_5 - \frac{0.895A_2A_5}{A_3} + 1.79A_1A_5\right) \qquad (30)$$

This equation was derived from the Gräffe method. The corrected $\bar{A}_3$ is from 1 to 3.5 percent (on the average 1.5 percent) smaller than A_3. The error still possible is now smaller than 0.2 percent. Finally, the real parts of the two conjugate-complex pairs of roots are to be calculated with the aid of the Vieta relations for the entire frequency equation (20).

(b) Damping Times and Period of Oscillation of the Lateral Motions

The damping or excitation times and the period of oscillation of the lateral motions result from the roots of the frequency equation in the well-known manner. By damping time, we understand the time during which the motion is damped to the 1/e-fold value. $t_{\psi_1} = -T_F/\lambda_1$ is the damping time of the rolling motion, $t_{\psi_{23}} = -T_F/u_{23}$ the damping time of the yawing oscillation, $T_{\psi_{23}} = 2\pi T_F/w_{23}$ the period of oscillation of the yawing oscillation, $t_{\psi_{45}} = -T_F/u_{45}$ the damping or excitation time of the lateral displacement oscillation (> 0 indicates excitation time), $T_{\psi_{45}} = 2\pi T_F/w_{45}$ the period of oscillation of the lateral displacement oscillation. An important parameter for the judgment of an oscillation is, furthermore, $T_\psi/t_\psi = 2\pi u/w$, the number of oscillations to damp to the 1/e-fold value.

(c) Desirable Stability Properties in Towed Flight

In order to facilitate the work of the pilot, it was desired to obtain the following stability properties: 1. The lateral displacement oscillation is to be damped or at least indifferent. 2. The period of oscillation is to be as large as possible. 3. Static directional stability in towed flight is to be only small. As shown by the calculations, a high static directional stability in towed flight is always combined with a pronounced excitation of the lateral displacement oscillation. Furthermore, a high static stability decreases the control effectiveness. 4. Finally, a maximum damping and maximum period of oscillation of the yawing oscillation are desired, just like for an untowed airplane.

6. NUMERICAL CALCULATION OF THE DIRECTIONAL STABILITY

The directional instability in towed flight, in the shape of an excited lateral displacement oscillation, appears in a particularly intensive form in the case of the airplane Go 242[14] (fig. 6) with high wing loading, selected for the calculation of examples. Furthermore, detailed

[14]With this model, the author was able to collect detailed flight experiences for various climatic conditions and loading conditions. For unfavorable conditions, for instance, with high pay load and at high temperatures when the engine power fell off, or in the case of small airfields where the pilot was forced to lift off the ground too early, numerous false starts resulted which frequently led to failure of the airplane.

six-component measurements[15] exist for the Go 242, so that one may refer, not only to estimated or approximate calculated values, but also to measured values of aerodynamic force coefficients. The following calculations were performed:[16] Starting from a theoretical coupling at the center of gravity and an infinite length of cable, we investigated the influence of the position of the towing point and of the cable length on the origin of the conjugate-complex pair of roots λ_{45} of the lateral displacement oscillation and of the real root λ_6. Then the effects of the most important parameters of the flight attitude and of several configuration parameters on the directional stability were determined. Finally, the stability regions for variable flight mechanical and configuration parameters were determined with the aid of Routh's stability criteria.

(a) Influence of the Cable Length and of the Position of the Towing Point on the Origin of the Lateral Displacement Oscillation and on the Static Stability in Towed Flight

The approximate formulas for the roots offer a certain clue for recognizing the influence of individual coefficients on certain roots. A survey of the structure of the coefficients themselves is obtained if one breaks them down into the determining factors of table I.

An airplane towed with infinite cable length and the towing point situated at the center of gravity, is distinguished from the untowed airplane only by a variation of the spiral root λ_4 which in towed flight, due to the cable force, becomes negative and therefore stable. The coefficients A_5 and A_6 and the roots of the lateral displacement oscillation are not yet in existence. If one lets the cable length become finite (fig. 8), there newly originates the coefficient A_5, and from the root λ_4 a conjugate-complex pair of roots develops which characterizes the lateral displacement oscillation. The oscillation here is still damped. Therein $2u_{45} = \lambda_4$, that is, the damping of the oscillation is half as large as the real root for infinite cable length from which the oscillation arises. The period of oscillation is infinite

---

[15] H. Göthert, Sechskomponentenmessungen an dem Windkanalmodell Go 242, Unpublished report No. 82228 of the Luftfahrtforschungsantstalt Braunschweig, 1943; F. W. Scholkemeier, Weitere Sechskomponentenmessungen an dem Windkanalmodell Go 242, unpublished report No. 82239 of the Luftfahrtforschungsanstalt Braunschweig, 1943.

[16] The airplane data, parameters, coefficients, and roots of the frequency equation compiled in the tables had to be omitted. Reference is made to the dissertation of the author, Braunschweig 1947.

for infinite cable length. In fact, it attains relatively large values for very large cable lengths, for instance, $k_s = 24$, cable length $l = 290$ m, period of oscillation is 123 sec.

If one then lets the towing point deviate from the center of gravity horizontally up to the nose, one obtains the new coefficient A_6 and the static-stability root λ_6 which increases at first rapidly and then more slowly (fig. 9). The excitation increases about proportionally to it. The oscillation frequency grows in the same region to somewhat more than double its value. If one lets the towing point deviate from the center of gravity vertically up to the upper surface of the wing, A_6 and λ_6 will likewise originate (fig. 9). The excitation grows in proportion, and the oscillation frequency increases; however - corresponding to the smaller distances - not as much as in the case of the towing point travelling toward the nose.

(b) Influence of the Cable Length, of the Flight Attitude, and of Configuration Parameters on the Stability in Towed Flight

1. Variation of the towing-cable length[17].- The relative cable length was varied from 3 to 12, corresponding to an absolute cable length l of 36.7m to 147m. The relative cable lengths exceeding

[17]Transition to cable length 0: In the transition to a very short towing cable, the cable angle σ may become very large also for very small lateral-displacement and yawing oscillations. Then, however, the approximation for σ (5) is no longer correct. If, finally, l becomes zero, a free yawing oscillation about the center of gravity of the towed airplane is no longer possible. This case may be expressed by the two differential equations of the rolling motion and of the motion about the towing point on the towing airplane (coupled yawing and center-of-gravity path motion). Similar to the case $l = 0$ is the Fieseler rigid-bar tow (H. Solf, Jahrbuch 1942 der deutschen Luftfahrtforschung, p. I 391 and K. Petrikat and E. Pieruschka, Jahrbuch 1942 der deutschen Luftfahrtforschung, p. I 404) and the three-point tow (W. Söhne, Die Seitenstabilität eines geschleppten Flugzeuges. Der Dreiecksschlepp, Monography of the M.O.S. Völkenrode, 1946) where, due to the two cables acting, at a larger distance, on the wing nose, a free yawing oscillation is no longer possible, either.

these amounts $k_s = 24, 48, 96$ have only a theoretical significance and were investigated in order to observe the origin of the lateral displacement oscillation. With increasing cable length, the damping in roll λ_1, and the yawing oscillation $u_{23} + iw_{23}$ remain almost unchanged; excitation and frequency of the lateral displacement oscillation $u_{45} + iw_{45}$ and static stability in towed flight λ_6, in contrast, decrease (fig. 10). An increase of the length of the cable as a means for obtaining better stability, however, is advisable only up to a cable length of about $k_s = 6$ (76m). For reasons of practical flight operation, a short towline is desirable. A cable length of $k_s = 5 - 6$ (60 - 74m) seems therefore to be most favorable.

2. Variation of the lift coefficient.- Here we calculated with six different c_a values from 0.303 to 1.0, in order to cover the entire lift range. The lift coefficients above 0.681 appear, in practical flight operation, generally only in the unsteady accelerated flight after the take-off. With increasing lift coefficient, the excitation u_{45} and the frequency w_{45} of the lateral displacement oscillation as well as the static stability in towed flight λ_6 increase. The period of oscillation $T_{\psi_{45}}$ slightly increases, up to the lift coefficient 0.6, and then again decreases slightly whereas the excitation time $t_{\psi_{45}}$ decreases considerably percentagewise (fig. 11). The pilot of the towed airplane is forced to balance by control deflections the instability which increases with increasing lift-coefficient values while simultaneously the effectiveness of the control surfaces decreases in proportion with the decreasing dynamic pressure. This is a difficult and very tiring task, particularly in squally weather. It explains the high degree of dependence of the stability on the flight speed. The calculation therefore confirms the flight experience according to which a directionally unstable airplane can no longer be controlled, above a certain lift coefficient (for Go 242, for instance, $c_a > 0.8$), in towed flight, although it exhibits, for this lift coefficient, still very satisfactory properties in untowed flight.

3. Variation of the flying weight.- Of the possible actual loading conditions, we selected as examples the empty flying weight with trimming ballast of 4,200 kg, the standard flying weight of 5,500 kg, and the full-loading flying weight of 6,800 kg. With increasing flying weight, the excitation and frequency of the lateral displacement oscillation and also the static stability increase very considerably. For the excitation time and period of oscillation as well as for the damping time of the static stability there results a slight decrease, due to the influence of the

flight-mechanical time unit T_F (fig. 12). With increasing weight, the c_a values, however, increase; the control effectiveness, therefore decreases. Furthermore, the reserve power of the towed airplane decreases, and the flight speed is therefore lower than in the case of smaller weight. The impediments resulting from the increase in lift coefficient appear therefore once more, in addition. The difficulties for the pilot in balancing the excitation increase, therefore, considerably more than is expressed in the amounts of the excitation times and period of oscillation.

4. Variation of the angle of climb.- The angles of climb selected as examples $\gamma = 3.44^\circ$ and 6.85° correspond, for $G = 5{,}500$ kg and $c_a = 0.681$ to the climbing speeds 2.8 m/s and 5.6 m/s. With increasing climbing speed, the excitation time of the lateral displacement oscillation and the static stability in towed flight decrease only slightly (fig. 13). The frequency of the lateral displacement oscillation, in contrast, increases considerably with increasing climbing angle, that is, the period of oscillation decreases which is a phenomenon that is likewise inconvenient for the pilot. Since climbing flight is, of course, always combined with a lower flight speed, here again the phenomena of the increasing excitation of the lateral displacement oscillation in low-speed flight and of the decreasing period of oscillation in climbing flight are additive. The calculation, therefore, confirms in this case, too, the flight experiences which show precisely for climbing flight at low speed the maximum instability and therewith the greatest difficulties in controlling the airplane.

5. Variation of the rolling moment due to sideslip by variation in dihedral.- The dihedral was varied from $+6.7^\circ$ to -5.3° whereby the rolling moment due to sideslip changed from $c_{l\beta} = -0.26$ to $+0.09$. With decreasing dihedral, the excitation u_{45} of the lateral displacement oscillation decreases more and more, and after the zero point has been passed, it turns into a rapidly increasing damping (figs. 14 and 15). The frequency of the oscillation shows a minimum for excitation zero and then increases again. The static stability decreases about proportionally with the excitation of the lateral displacement oscillation and makes the transition to the unstable region at approximately equal dihedral. From this remarkable dependence of the directional stability in towed flight on the rolling moment due to sideslip, one may draw the following conclusion: The optimum flight properties result in the case of coupling at the nose for a rolling moment due to sideslip $c_{l\beta} = 0$; for this moment the excitation of the lateral displacement oscillation is very small, the period of oscillation shows a maximum, and the static directional stability in towed flight simultaneously has become zero. For a high-wing monoplane, the rolling moment due to sideslip disappears at a slightly negative dihedral (Go 242: $\nu = -2.23^\circ$). It is true that the

airplane in untowed flight then shows a certain tendency toward spiral dive which is, however, unimportant since the untowed flight always lasts only a few minutes. The primary object of consideration for a towed airplane always is towed flight.

6. Variation of the vertical-tail surface area.- The vertical-tail surface area was increased from 2×3.85 to $2 \times 5.39 m^2$ in the manner indicated in figure 6 whereby the lateral force due to sideslip, the yawing moment due to sideslip, and the damping in yaw increased considerably. To increase the vertical-tail surface area is a customary means for improving the directional stability of an untowed airplane. In the case of the towed airplane, there results likewise a large increase in damping, but - it is true - also a slight increase in the frequency of the yawing oscillation. The excitation and frequency of the lateral displacement oscillation, in contrast, decrease only slightly (fig. 16); therefore excitation time and period of oscillation show a slight increase. For this reason, an increase in vertical-tail surface area would therefore hardly be a profitable means for improvement of directional stability in towed flight. However, the pilot has to balance the self-exciting lateral displacement oscillation by suitable aileron and rudder operation. This will be easier the more effective (and thus larger) these tail surfaces are. Thus, an increase in vertical-tail surface area is, after all, wholly suitable for improving the directional stability of a towed airplane.

7. Variation of the damping in roll.- In the case of a variation of the moment coefficient of the damping roll from $l_x = 15.12$ to 18.48 (as may be caused, for instance, by a variation in the aspect ratio of the wing from $\Lambda = 8$ to 13.1), the damping-in roll root λ_1 increases proportionally to the moment coefficient of the damping-in-roll l_x. The excitation and the frequency of the lateral displacement oscillation decrease slightly, the excitation time and period of oscillation therefore slightly increase (fig. 17). According to the calculation, the towing properties of an airplane with high damping in roll, that is, with high aspect ratio, are therefore somewhat more favorable than those of an airplane with low damping in roll, that is, low aspect ratio. On the other side, there is, of course, the greater inertia with which an airplane with higher aspect ratio reacts to aileron deflections.

8. Coupling at the lower side of the fuselage and variation in the position of the towing point in horizontal direction.- Indifference of the lateral displacement oscillation combined with static indifference may be obtained without variations in the configuration of the airplane when the towing point is placed on the lower side of the fuselage, ahead of the center of gravity. In the case of coupling vertically below the center of gravity at the lower side of the fuselage, there results static instability and a damped lateral displacement oscillation. If one then

lets the towing point travel forward to a position 0.90m ahead of the center of gravity, the root of the static stability λ_6 passes into a stable region. Simultaneously, the damped lateral displacement oscillation at this point becomes an excited oscillation (fig. 18) and the oscillation frequency shows a minimum. By coupling below the center of gravity, a tail-heavy moment is created which must be balanced by elevator trimming. A coupling at the lower side of the fuselage 0.90m ahead of the center of gravity seems, therefore, to be considerably more favorable than the customary coupling at the nose.

(c) Stability Limits for Various Cable Lengths, Weights, and Lift Coefficients Against the Rolling Moment Due to Sideslip

The variation of c_{l_β} for $G = 5{,}500$ kg, $c_a = 0.436$, $k_s = 6$ resulted, in the case of coupling at the nose, in a special dependence of static stability and of the excitation of the lateral displacement oscillation on c_{l_β}. It appeared therefore desirable to check this result for other weights, cable lengths, and lift coefficients as well. With the aid of Routh's stability criteria, we determined the stability limits for dynamic and static stability for these variables against the rolling moment due to sideslip. According to this, the limit of static stability lies at $l_\beta = 0$. For all weights the limit of static stability varies, as the cable length is decreased from a very small negative value to a somewhat larger positive value of l_β. However, the difference is so slight (approximately $1/4^\circ$ dihedral) that for all practical purposes, one may state that in the case of variation of the dihedral, for cruising flight $c_a = 0.436$ the limits of static and of dynamic stability coincide at $l_\beta = 0$ in such a manner that one can obtain either only static stability and dynamic instability or vice versa, or static and dynamic indifference. In contrast, a simultaneous variation of the lift coefficient and of the dihedral (fig. 19) shows that below a lift coefficient of $c_a = 0.42$, a gradually widening region of static and dynamic stability results. Above $c_a = 0.42$, there is a region of simultaneous static and dynamic instability.

7. SUMMARY

With the aid of the well-known directional-stability theory[18] (for untowed airplanes), the directional stability of an airplane towed by

[18] See footnote 4 on p. 4 and footnote 11 on p. 22.

means of a cable was theoretically investigated according to the method of small oscillations, and the frequency equation for it was derived. Whereas the frequency equation of the directional stability of an untowed airplane is an equation of the fourth degree, there results for the towed airplane an equation of the sixth degree. The damping-in-roll root λ_1 and the pair of roots of the yawing oscillation $\lambda_{23} = u_{23} \pm iw_{23}$ of the untowed airplane remain valid almost without modification whereas the spiral root λ_4, in contrast, disappears. In its place there appears a new conjugate-complex pair of roots $\lambda_{45} = u_{45} \pm iw_{45}$ which characterizes the lateral displacement oscillation occurring in towed flight, and a real root λ_6 which represents the static directional stability in towed flight. The lateral displacement oscillation is generally excited. The limit of dynamic stability may be determined by the Hurwitz-Routh stability criteria. We investigated what discriminant is decisive for the stability limit of the lateral displacement oscillation, and found that it was possible to simplify the corresponding expression considerably. The investigation of special cases in which one or two degrees of freedom (rolling and yawing oscillation) had been neglected did not yield usable approximate solutions.

Numerous examples were calculated for the airplane Go 242. For coupling at the center of gravity, if one passes from infinite cable length to a cable length which is finite, there originates a damped oscillation from the real root λ_4. If the towing point deviates from the center of gravity in the horizontal direction forward or in the vertical direction upward, this oscillation becomes an excited oscillation and its frequency increases. Simultaneously, there appears a real root which represents the static stability in towed flight. Then various parameters of flight attitude and configuration were varied. It was found that in the present model the lateral displacement oscillation is strongly excited. Its duration amounts to 19 to 32 seconds, according to the cable length, thus to about the 7- to 10-fold multiple of the yawing oscillations. The most noteworthy results of a variation of the individual parameters are:

1. With increasing cable length, the frequency and excitation of the lateral displacement oscillation decrease. However, it is not worthwhile to increase the cable length beyond $k_s = 6$ ($l = 76$m).

2. With increasing lift coefficient, the excitation and frequency of the lateral displacement oscillation increase.

3. The same occurs in the case of increasing pay load.

4. With increasing angle of climb, only the frequency of the lateral displacement oscillation increases.

These results confirm the flight experiences and flight measurements and explain many difficulties in towed flight and accidents that have occurred. They are probably similar for other model types with a high wing loading.

5. In the case of variation of the dihedral, the excitation of the lateral displacement oscillation reverts, for a vanishing rolling moment due to sideslip ($\nu = -2.23^{\circ}$) to zero, the period of oscillation here attains a maximum. Simultaneously, the static stability in towed flight becomes equal to zero. With the aid of the Routh discriminant, the stability limits against the rolling moment due to sideslip were determined also for other weights, cable lengths, and lift coefficients. There resulted below $c_a = 0.42$ a region of simultaneous static and dynamic stability. For this structural design (namely $l_\beta = 0$ to 0.2, $\nu = -2^{\circ}$ to 2.3°), the towing conditions are therefore the most favorable ones. An absolute stability in towed flight in the sense that the airplane is controlled by the cable forces and moments in such a manner that the pilot's work is made completely superfluorous is unattainable. For $l_\beta > 0$ the lateral displacement oscillation is damped, but static instability exists whereas for $l_\beta < -0.2$ static stability exists, the lateral displacement oscillation, however, is excited.

6. With increasing area of the vertical-tail surfaces, the frequency and excitation of the lateral displacement oscillation decrease only little; however, under certain circumstances such an increase may be advisable for improvement of the control effectiveness.

7. An increase in the moment coefficient of damping in roll l_x yields a small decrease of excitation and frequency of the lateral displacement oscillation.

8. In the case of coupling at the lower side of the fuselage 0.90m ahead of the center of gravity, static and dynamic indifference may likewise be attained without configuration changes in the airplane. This position of the towing point seems therefore to be more favorable than the customary coupling at the nose.

Translation by Mary L. Mahler
National Advisory Committee
for Aeronautics

TABLE I.- COEFFICIENTS OF THE STABILITY EQUATION, ARRANGED ACCORDING TO DETERMINING FACTORS WITH NUMERICAL EXAMPLE FOR $G = 5{,}500$ kg; $k_s = 6$; $c_a = 0.436$

	A_A	ΔA_s	ΔA_F	ΔA_l	ΔA_{lF}
$A_1 =$	$l_x + n_z + c_{q\beta} - c_a \tan\gamma$ 18.70	c_s 0.037			
$A_2 =$	$l_x n_z - n_x l_z +$ $(c_{q\beta} - c_a \tan\gamma)(l_x + n_z) + \mu_s n_\beta$ 49.76	$c_s(l_x + n_z)$ 0.67	$n_s\mu_s\left(1 + \frac{a}{l}\right)$ 1.89	$c_s\frac{\mu_s}{k_s}$ 0.07	
$A_3 =$	$(c_{q\beta} - c_a \tan\gamma)(l_x n_z - n_x l_z) +$ $\mu_s\left[l_x n_\beta - n_x l_\beta - c_a(l_\beta + n_\beta \tan\gamma)\right]$ 280.6	$c_s(l_x n_z - n_x l_z) +$ $c_s\mu_s n_\beta\left(1 + \frac{a}{l}\right)$ 1.54	$\mu_s\left(1 + \frac{a}{l}\right)\left[n_s(l_x +$ $c_{q\beta} + c_w) - l_s n_x\right]$ 32.7	$c_s\frac{\mu_s}{k_s}(l_x + n_z)$ 1.78	
$A_4 = \mu_s$	$\left\{c_a\left[n_\beta l_z - l_\beta n_z - \tan\gamma(l_x n_\beta - n_x l_\beta)\right]\right.$ -4.97	$c_s\left(1 + \frac{a}{l}\right)(l_x n_\beta - l_\beta n_x)$ 9.52	$\left(1 + \frac{a}{l}\right)(n_s l_x - n_x l_s)(c_{q\beta} + c_w)$ 15.45	$\frac{c_s}{k_s}(\mu_s n_\beta + l_x n_z - n_x l_z)$ 2.92	$\frac{\mu_s}{k_s}\left[(c_{q\beta} + c_s)n_s + c_a l_s)\right]\Big\}$ 1.75
$A_5 = \mu_s^2$			$\left\{c_a\left(1 + \frac{a}{l}\right)(n_\beta l_s - l_\beta n_s)\right.$ 21.08	$\frac{c_s}{k_s}(l_x n_\beta - n_x l_\beta)$ 18.09	$\frac{1}{k_s}\left[(c_{q\beta} + c_s)(l_x n_s - n_x l_s) +\right.$ $\left.c_a(n_z l_s - l_x n_s)\right]\Big\}$ 34.87
$A_6 = \mu_s^3$					$\left\{\frac{c_a}{k_s}\left(1 + \frac{a}{l}\right)(l_s n_\beta - n_s l_\beta)\right\}$ 40.0

A_A = coefficients for the untowed airplane

ΔA_s = additional term, stemming from the cable force, for towing point at the center of gravity, but independent of the cable length

ΔA_F = additional term, stemming from the cable moments, but independent of the cable length[19]

ΔA_l = additional term, stemming from the cable force at the center of gravity due to finite cable length

ΔA_{lF} = additional term, stemming from cable moments due to finite cable length

[19] In the case of coupling at the nose, for $c_a = 0.56$, the towing point lies at the same height as the center of gravity. Hence, h_s and $l_s = 0$. For other angles of attack, too, l_s remains small compared to n_s, and was neglected for the sake of simplification of the calculation.

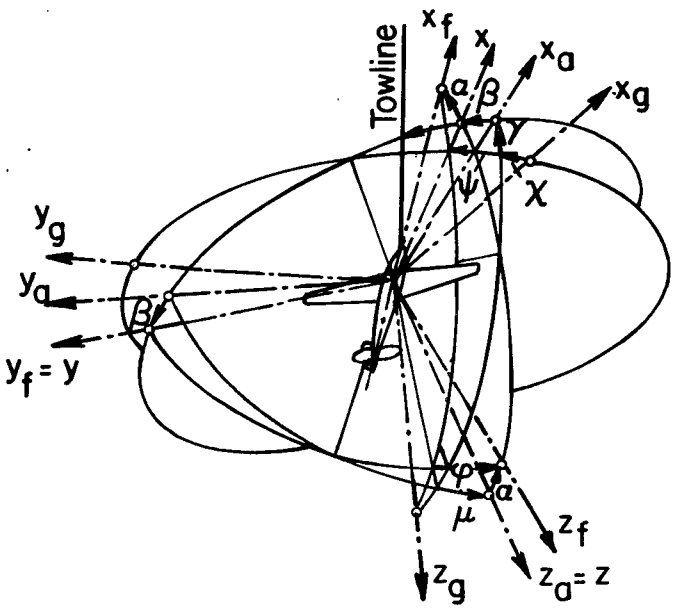

Figure 1.- Coordinate systems of the towed airplane. (The NACA reviewer suggests that the angle between the towline and x in the xy-plane should be labeled $\sigma - \chi \cos \gamma - \beta$.)

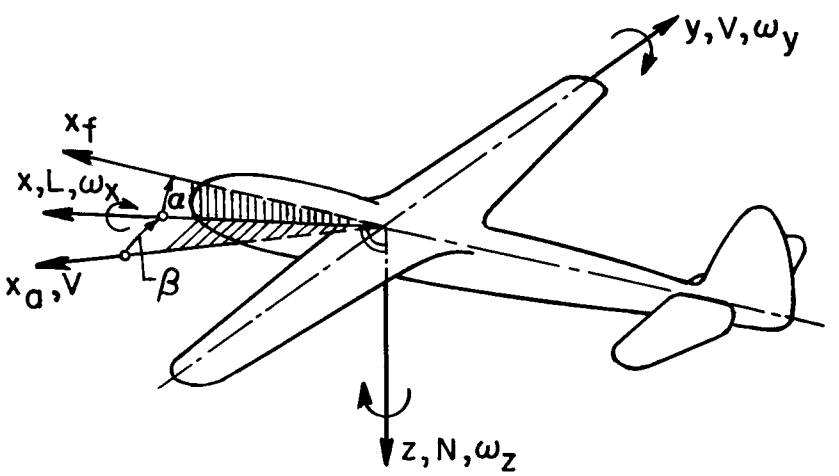

Figure 2.- Forces, moments, and motions of directional stability.

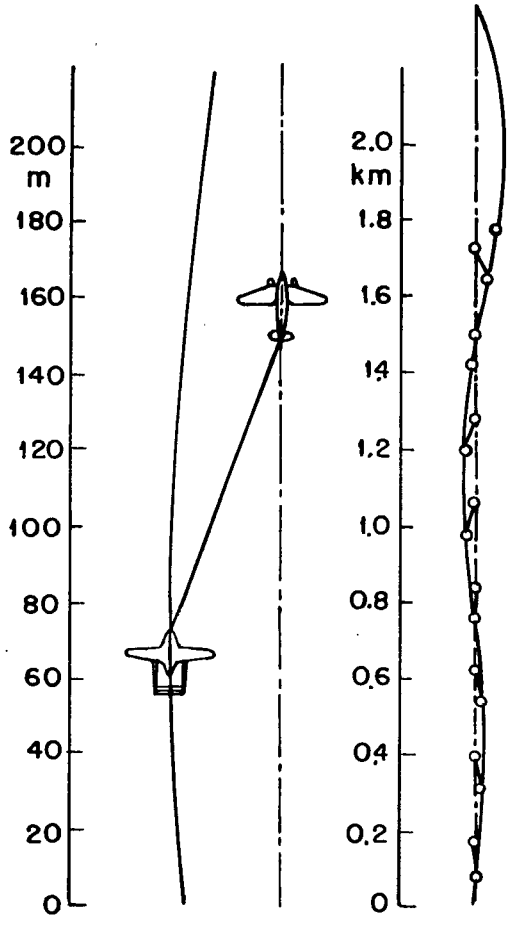

Figure 3.- Excited lateral displacement oscillation of a towed airplane at a flight speed of 206 km/h and a cable length of 80 m. Towing airplane He 111, freight glider Go 242. Period of oscillation ~ 32 sec.

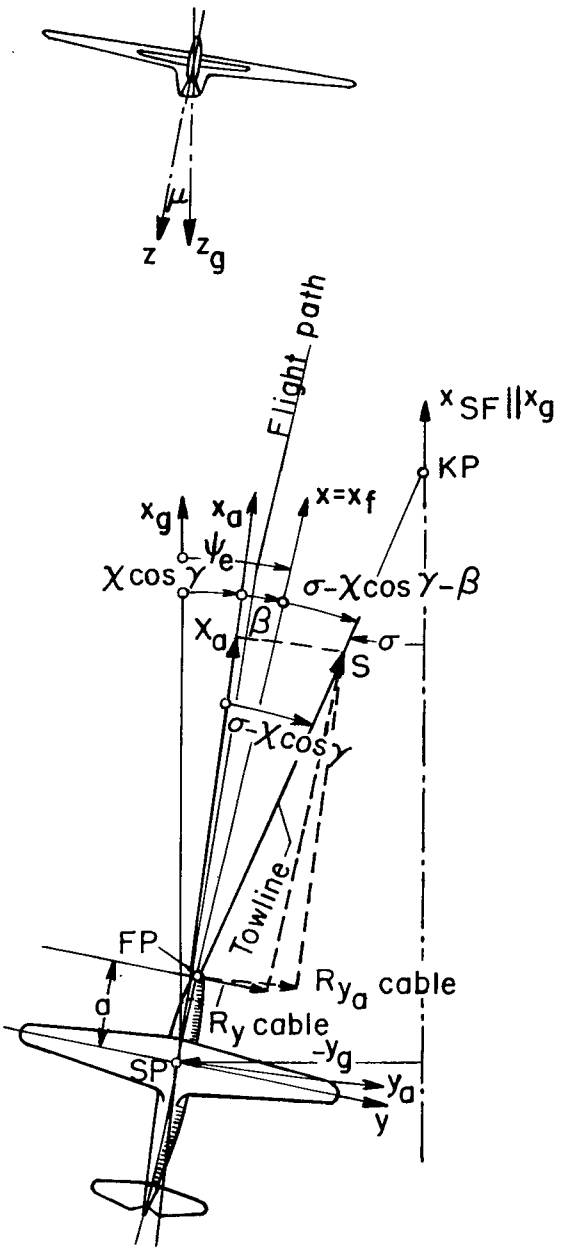

Figure 4.- Cable forces and angles on the towed airplane. KP coupling point on the towing airplane; SP center of gravity of the towed airplane; FP towing point on the towed airplane. (The NACA reviewer suggests that the labels x_a, R_{y_a} cable, R_y cable should possibly be R_{x_a}, S_{y_a}, and S_y, respectively.)

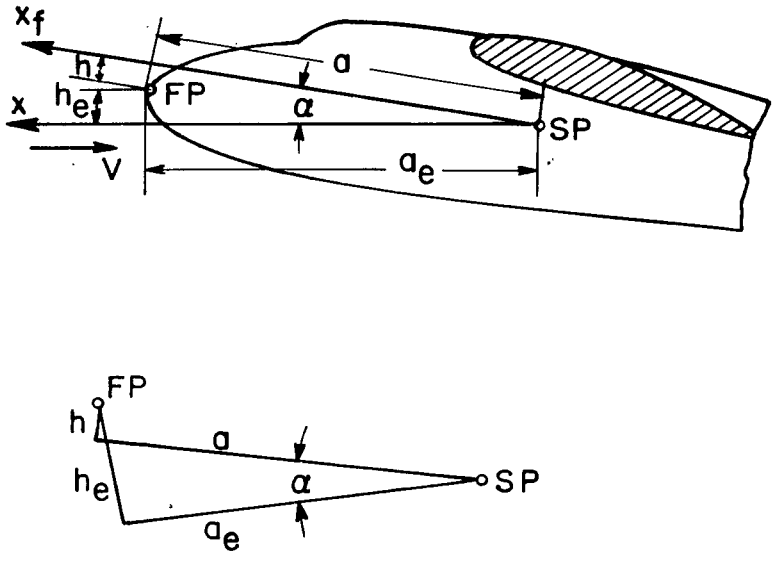

Figure 5.- Coordinates of the towing point on the towed airplane. $h > 0$ towing point above the center of gravity; $a > 0$ towing point ahead of the center of gravity (in the figure above, h is negative). $h_e = h \cos \alpha + a \sin \alpha$, $a_e = a \cos \alpha - h \sin \alpha$.

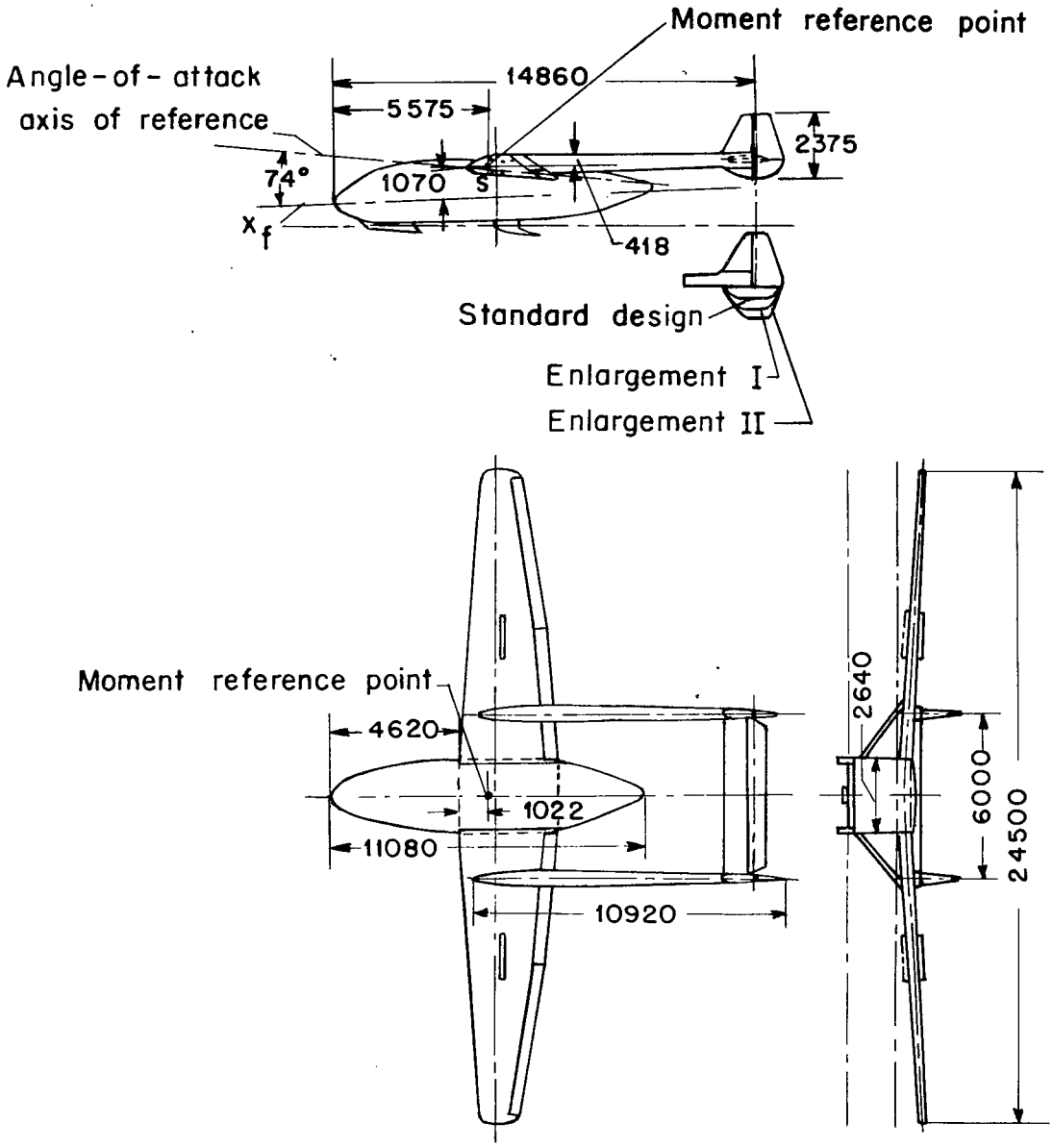

Figure 6.- General view of the freight glider Go 242.

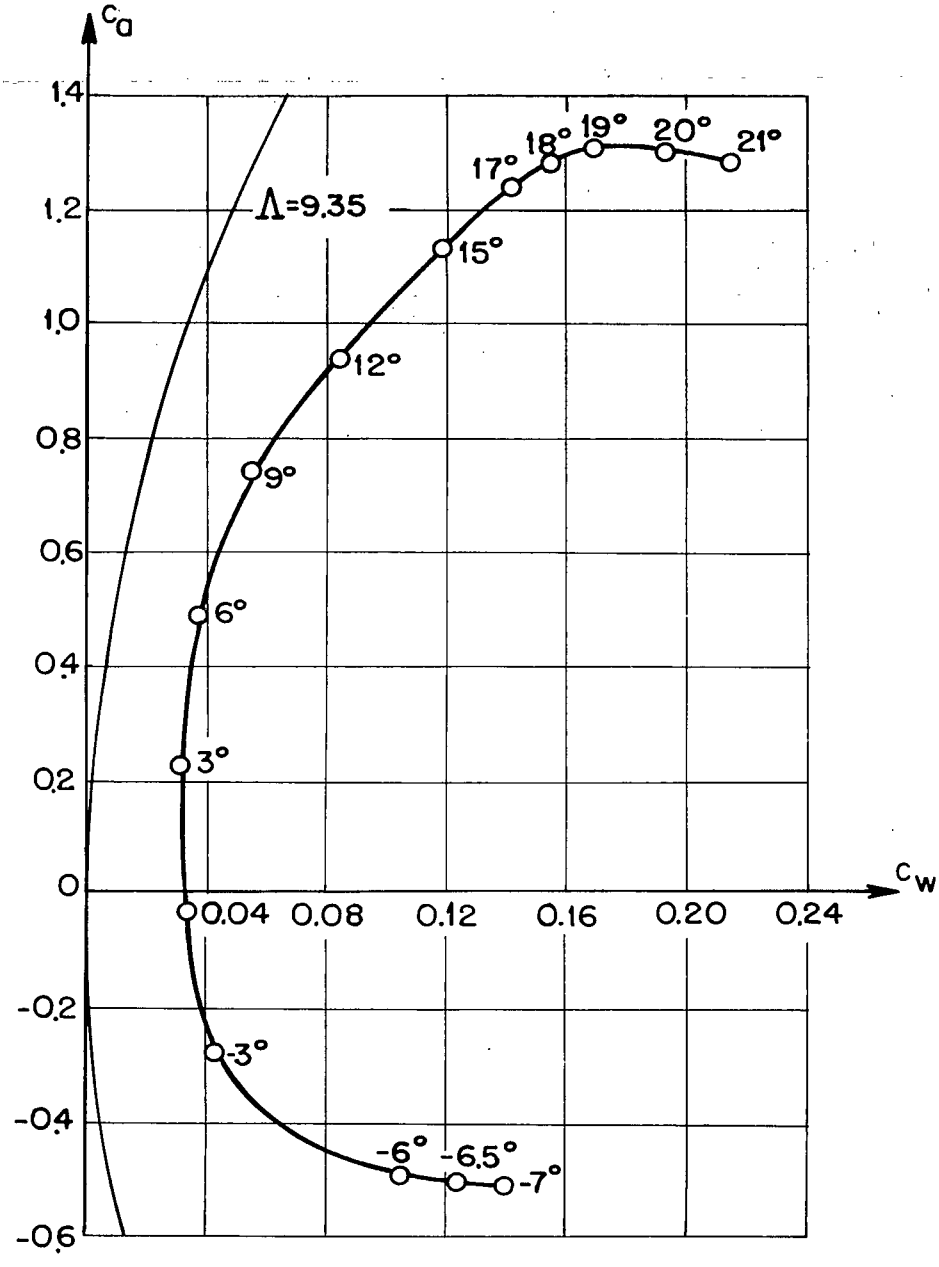

Figure 7.- Polar of the freight glider Go 242.

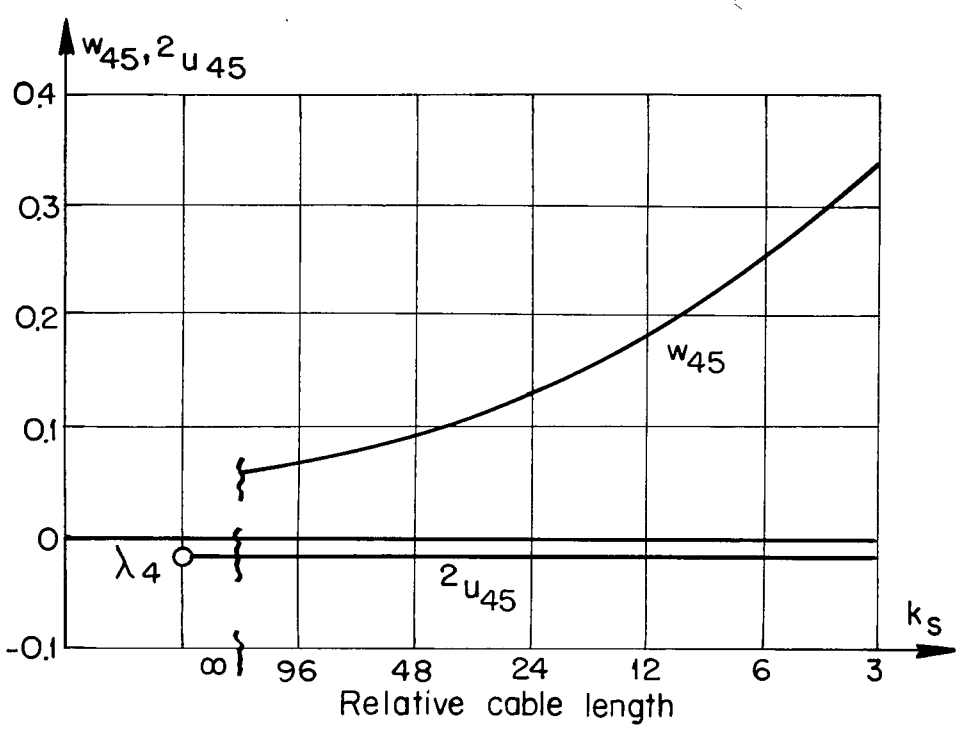

Figure 8.- Origination of the roots of the lateral displacement oscillation for change of the cable length from infinity and for coupling at the center of gravity. G = 5500 kg, c_a = 0.436.

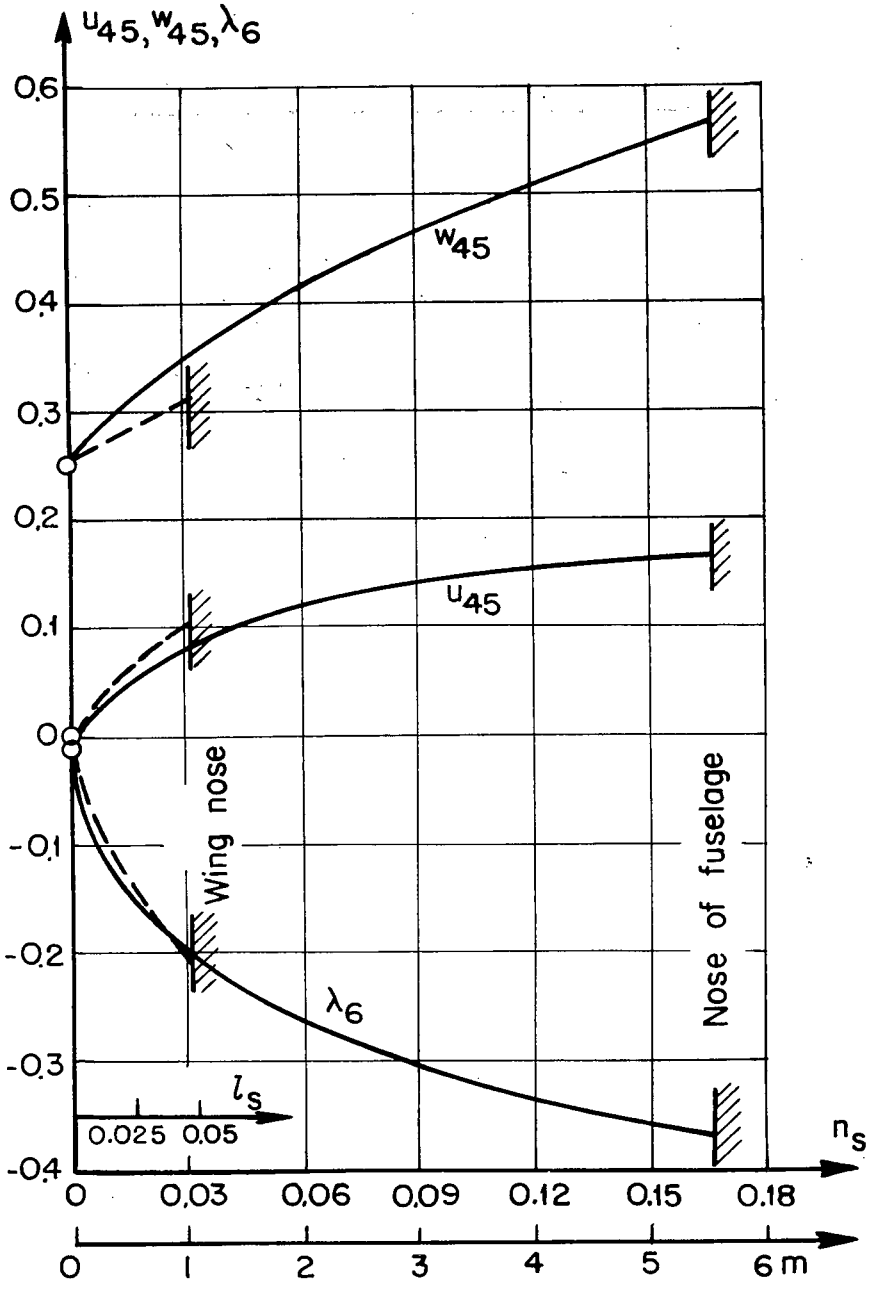

Figure 9.- Roots of the lateral displacement oscillation $u_{45} \pm iw_{45}$ and of the static stability λ_6 for variations in the position of the towing point (1) in horizontal direction from the center of gravity toward the nose of the fuselage, and (2) in vertical direction from the center of gravity toward the wing nose.

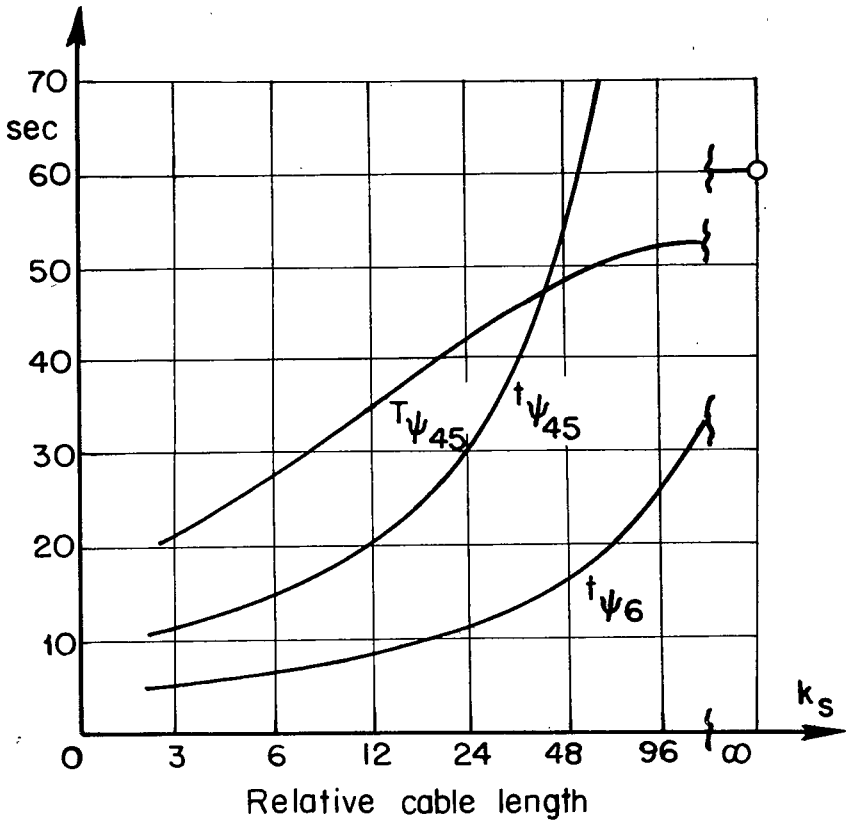

Figure 10.- Period of oscillation $T_{\psi_{45}}$ and excitation time $t_{\psi_{45}}$ of the lateral displacement oscillation and damping time of the static stability t_{ψ_6} in the case of variation of the cable length. G = 5500 kg, c_a = 0.436.

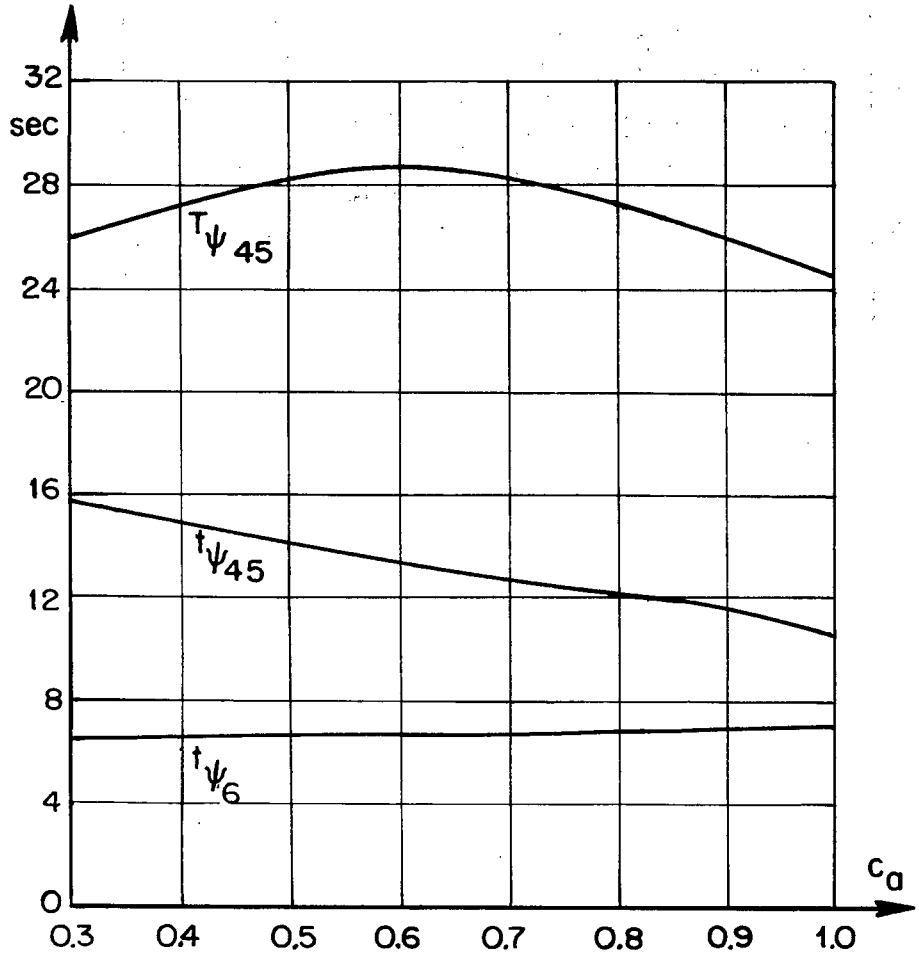

Figure 11.- Period of oscillation $T_{\psi_{45}}$ and excitation time $t_{\psi_{45}}$ of the lateral displacement oscillation and damping time of the static stability t_{ψ_6} in the case of variation of the lift coefficient.

G = 5500 kg, $k_s = 6$.

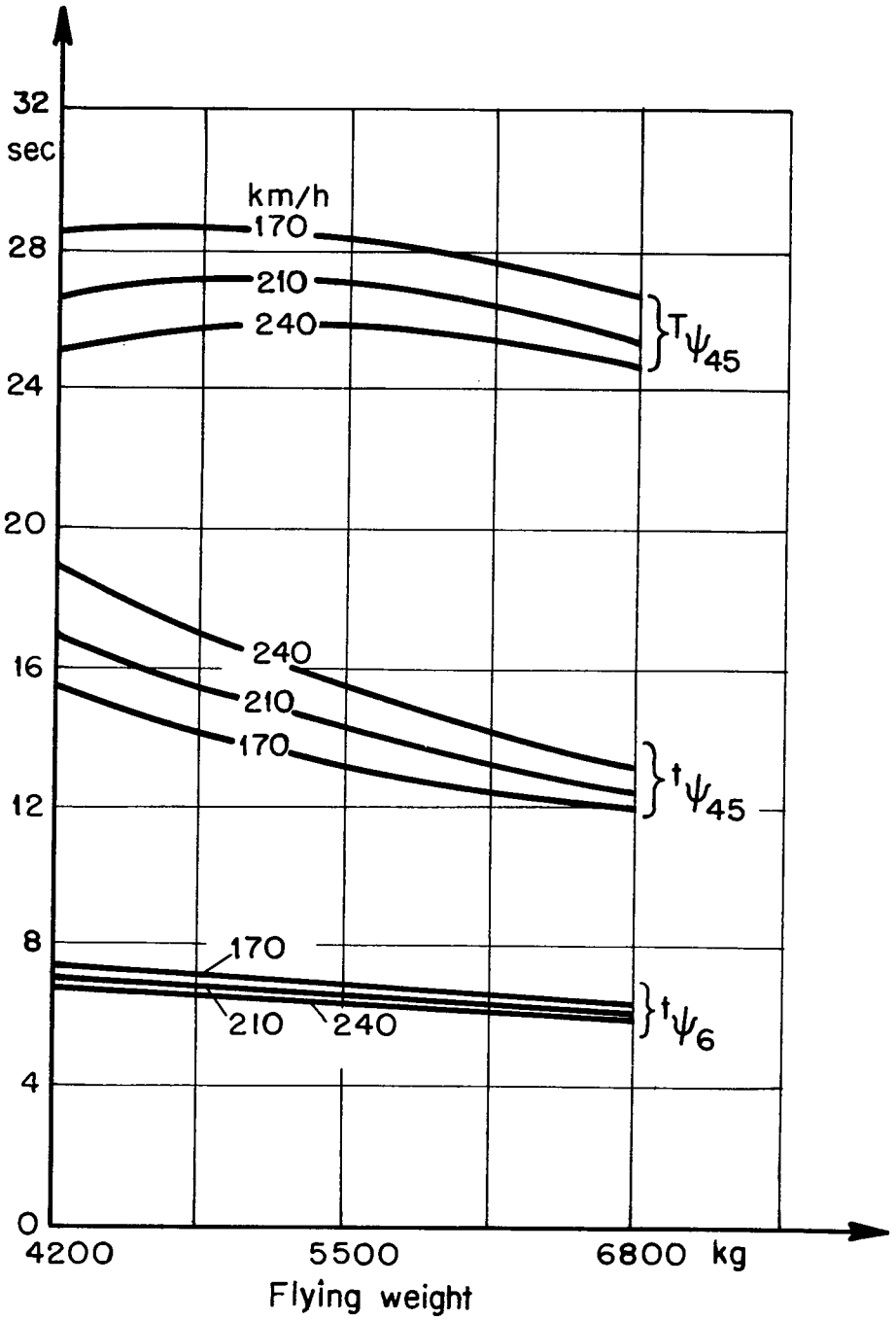

Figure 12.- Period of oscillation and excitation time of the lateral displacement oscillation and damping time of the static stability in the case of variation of the flying weight and for various flight speeds. $k_S = 6$.

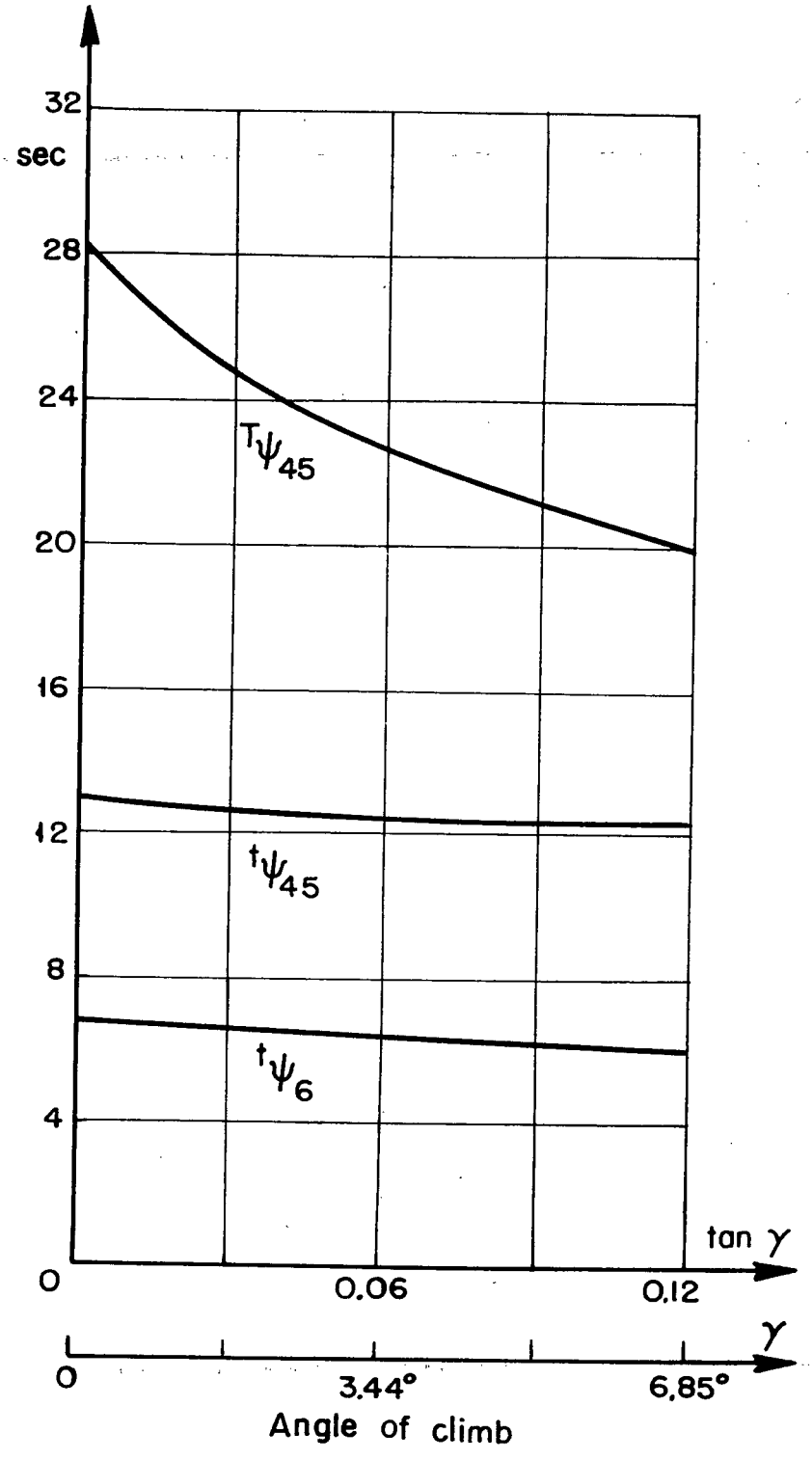

Figure 13.- Period of oscillation and excitation time of the lateral displacement oscillation and damping time of the static stability in the case of variation of the climbing angle. G = 5500 kg, $c_a = 0.681$, $k_s = 6$.

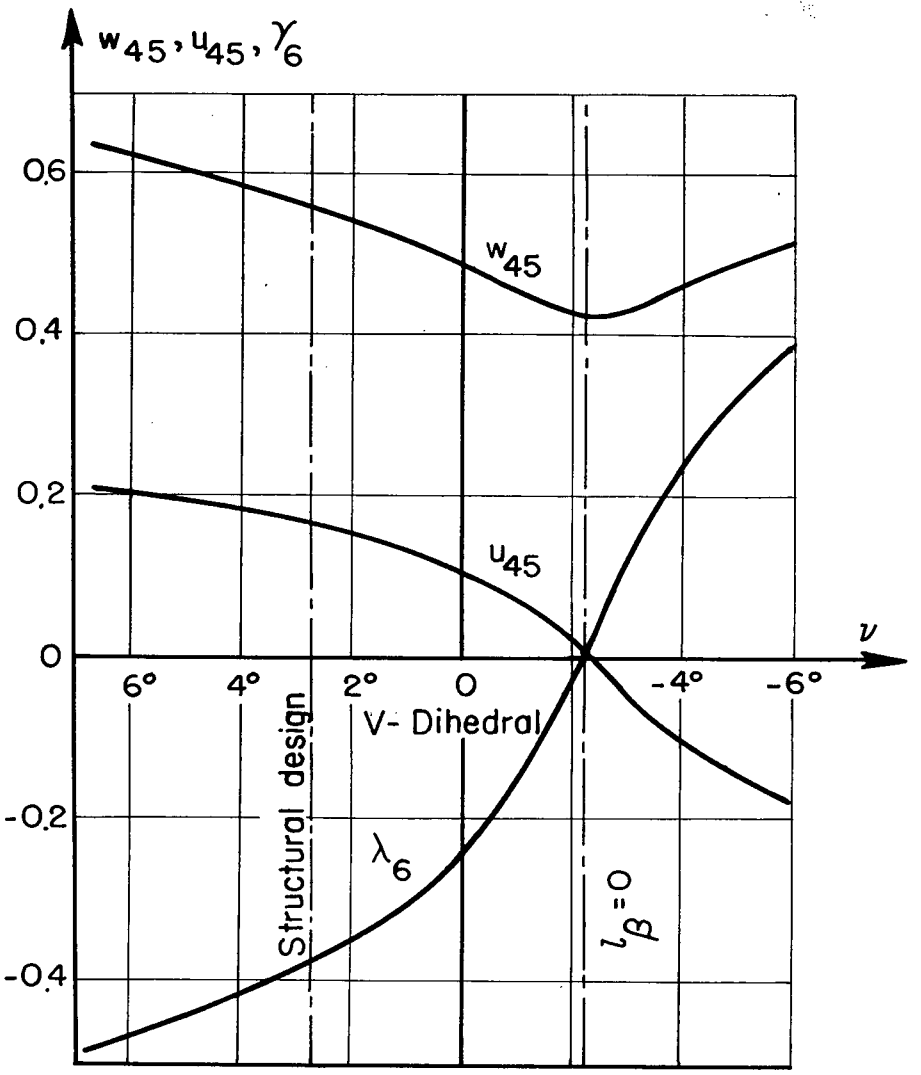

Figure 14.- Roots of the lateral displacement oscillation $u_{45} \pm iw_{45}$ and of the static stability λ_6 in the case of variation of the dihedral. G = 5500 kg, $c_a = 0.436$, $k_s = 6$.

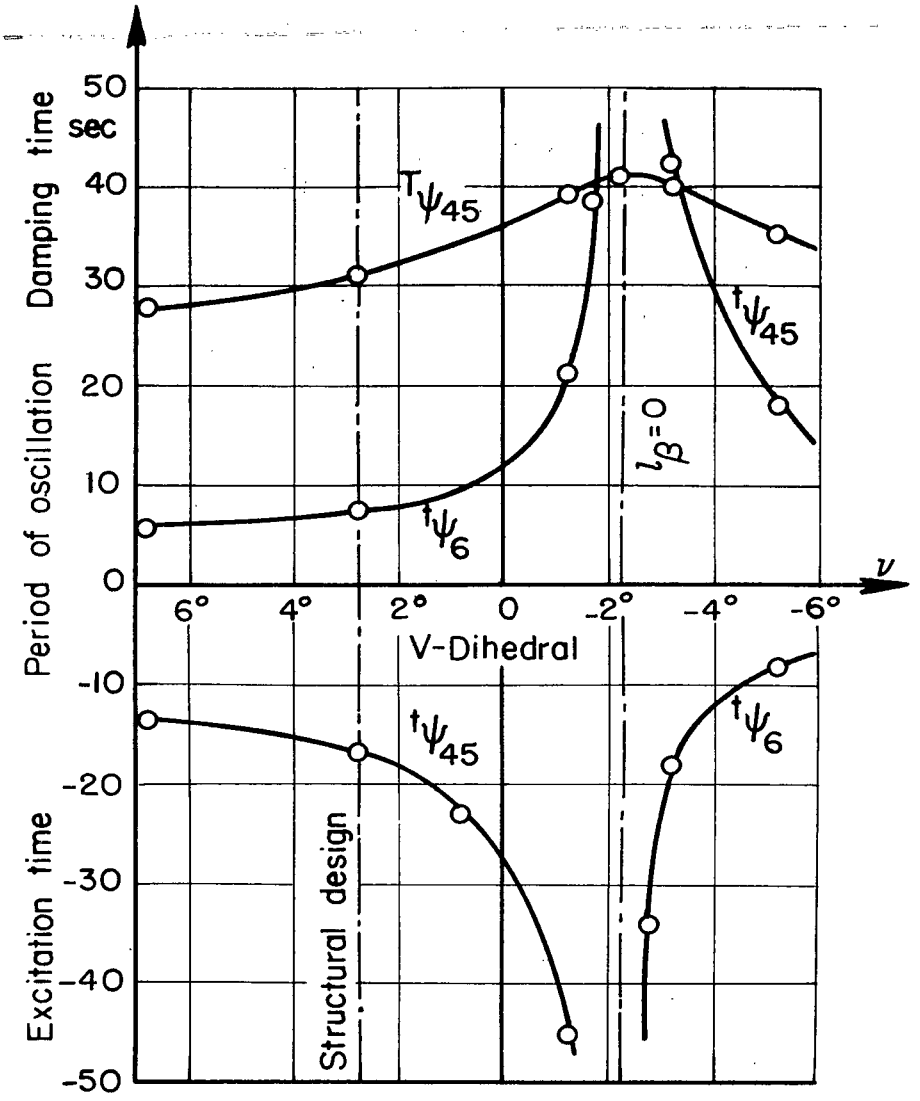

Figure 15.- Period of oscillation and excitation time of the lateral displacement oscillation and damping time of the static stability in the case of variation of the dihedral. G = 5500 kg, $c_a = 0.436$, $k_s = 6$.

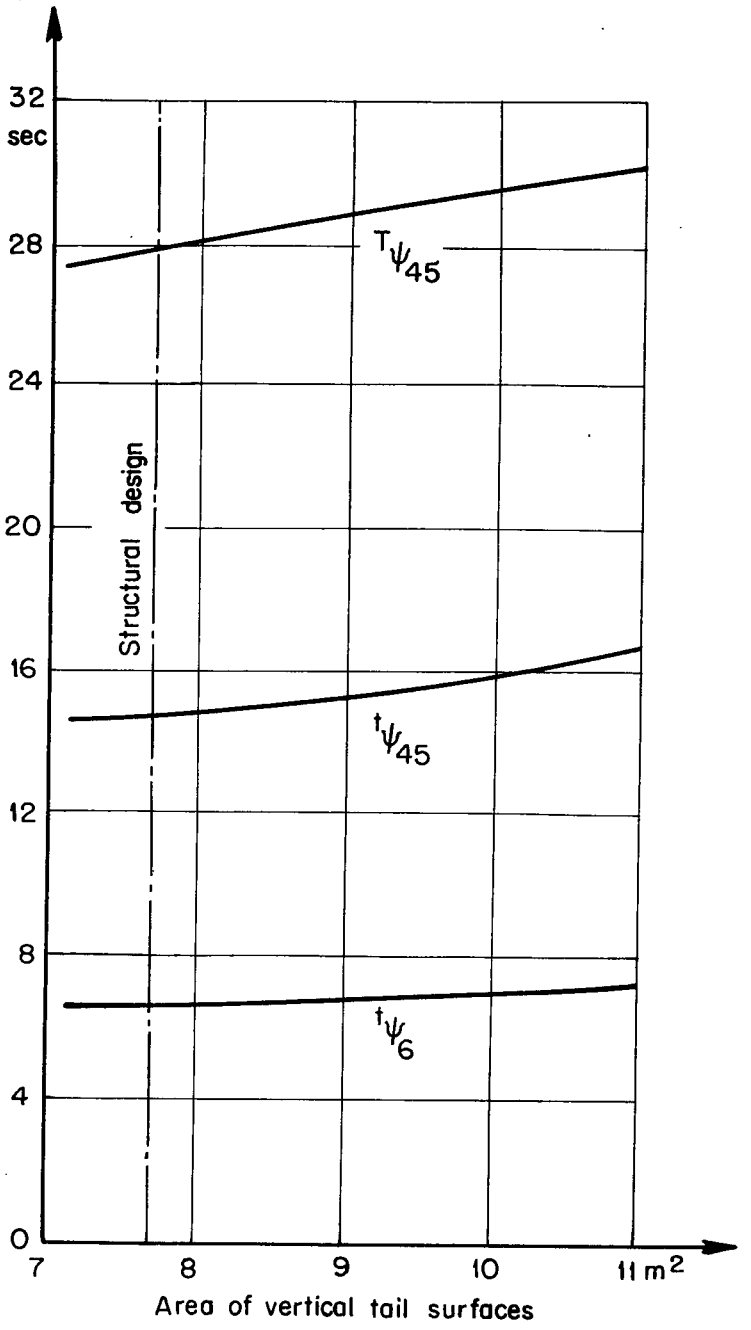

Figure 16.- Period of oscillation and excitation time of the lateral displacement oscillation and damping time of the static stability in the case of variation of the vertical-tail-surface area. G = 5500 kg, c_a = 0.436.

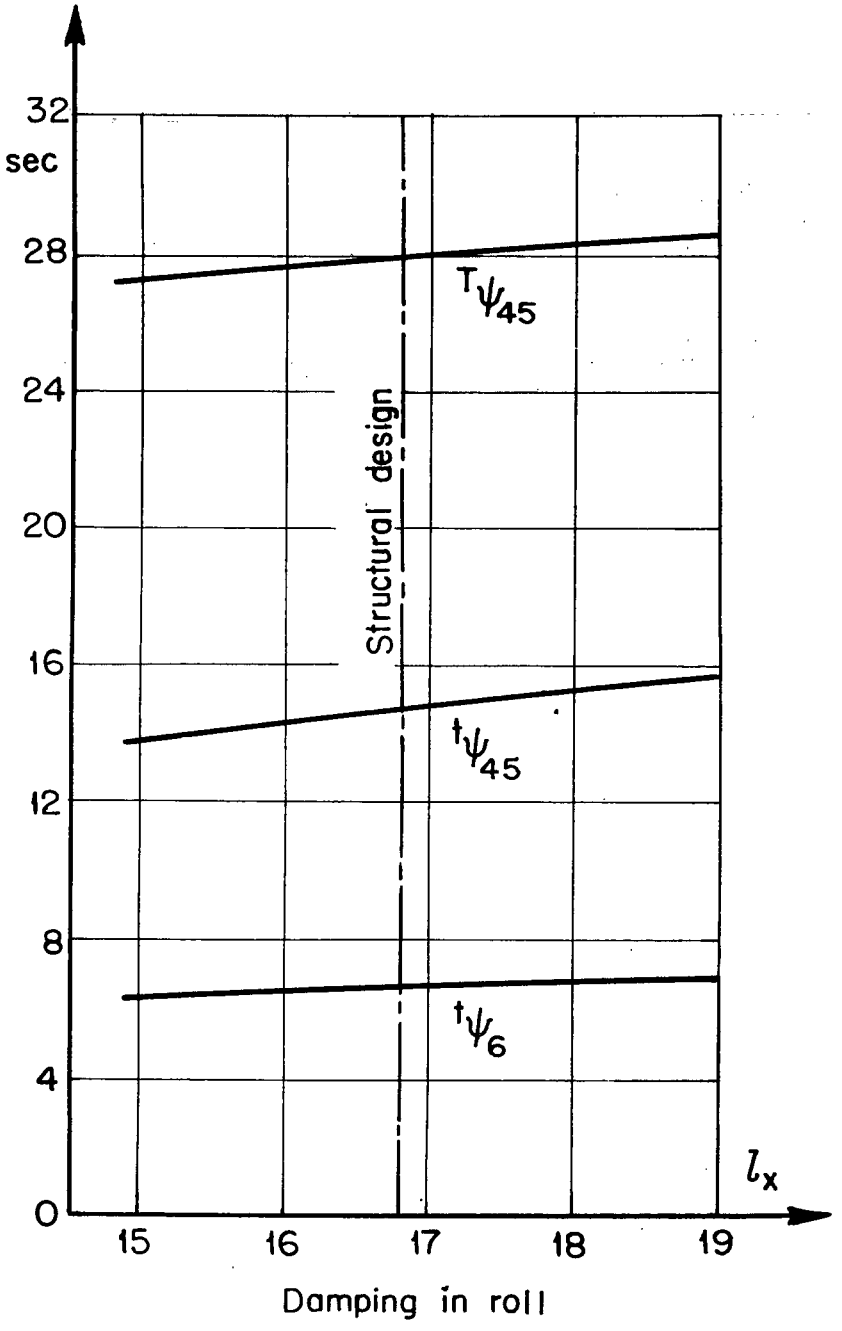

Figure 17.- Period of oscillation and excitation time of the lateral displacement oscillation and damping time of the static stability in the case of variation in damping in roll. G = 5500 kg, c_a = 0.436.

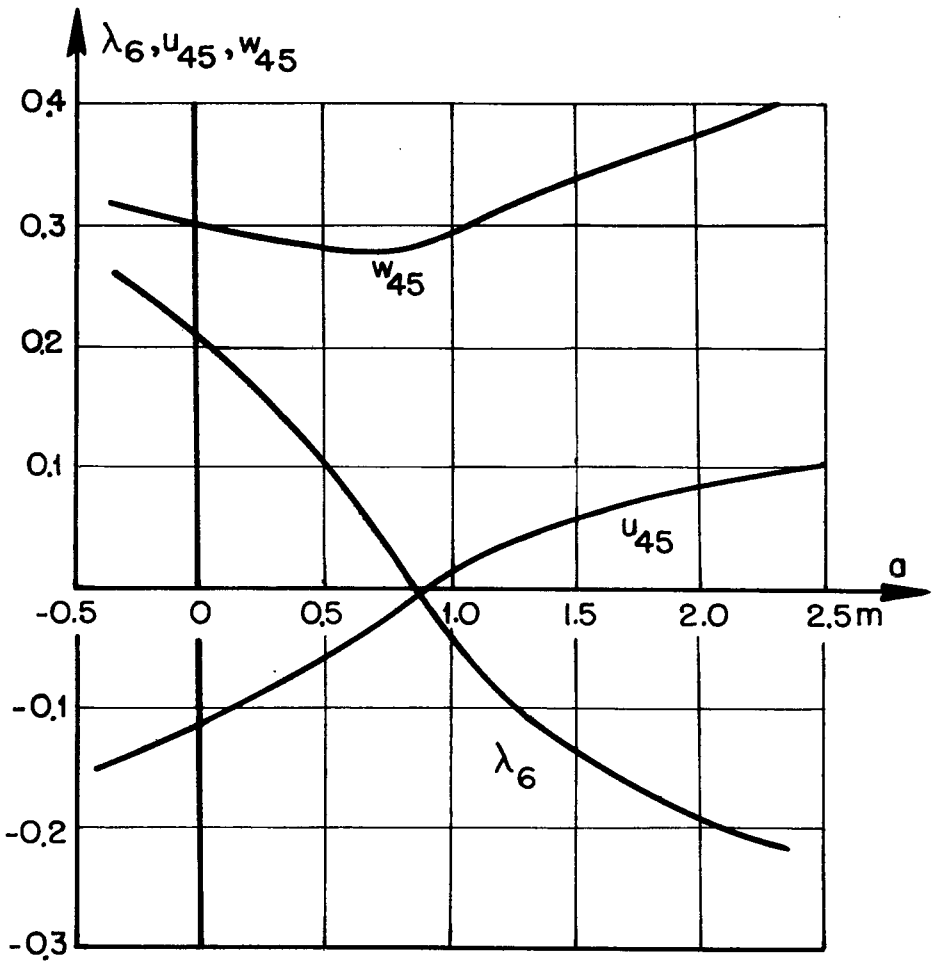

Figure 18.- Roots of the lateral displacement oscillation $u_{45} \pm iw_{45}$ and of the static stability λ_6 in the case of forward deviation of the towing point at the lower side of the fuselage. a = horizontal component of the distance from towing point to the center of gravity.

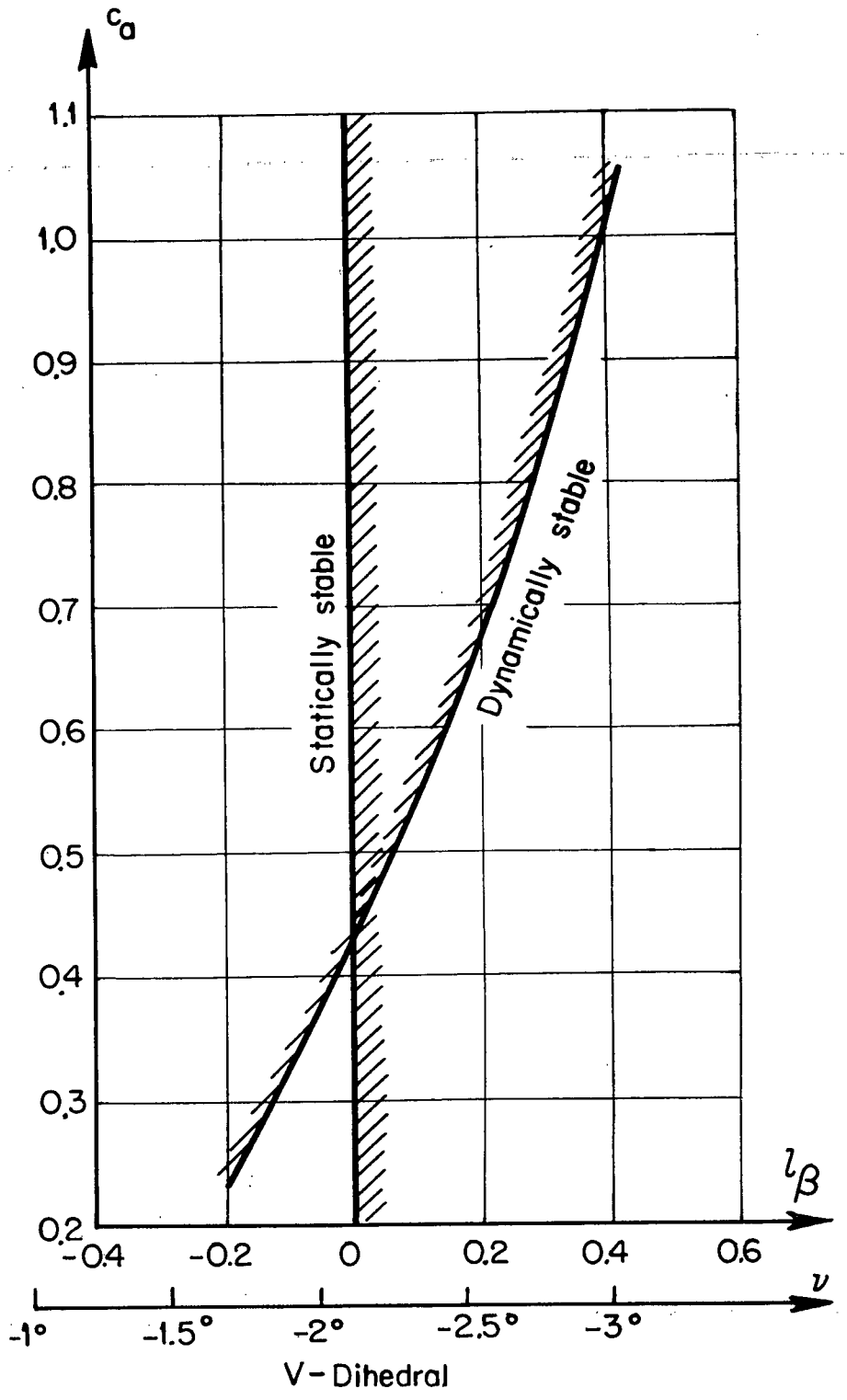

Figure 19.- Stability limits in the case of variation of the lift coefficient as a function of the dihedral.